Xu *et al. Microstructures* 2022;2:2022011
DOI: 10.20517/microstructures.2022.02

Microstructures

Review

Open Access

Check for updates

Recent advances in two-dimensional van der Waals magnets

Hang Xu[1,#], Shengjie Xu[1,#], Xun Xu[2,3], Jincheng Zhuang[1], Weichang Hao[1,3], Yi Du[1,3]

[1]School of Physics, Beihang University, Beijing 100191, China.
[2]Institute for Superconducting and Electronic Materials, University of Wollongong, Wollongong, NSW 2500, Australia.
[3]BUAA-UOW Joint Research Centre, University of Wollongong, Wollongong, NSW 2500, Australia.
[#]Authors contributed equally.

Correspondence to: Prof. Yi Du, School of Physics, Beihang University, No. 37 Xueyuan Road, Haidian District, Beijing 100191, China. E-mail: yi_du@buaa.edu.cn; Prof. Weichang Hao, School of Physics, Beihang University, No. 37 Xueyuan Road, Haidian District, Beijing 100191, China. E-mail: whao@buaa.edu.cn

How to cite this article: Xu H, Xu S, Xu X, Zhuang J, Hao W, Du Y. Recent advances in two-dimensional van der Waals magnets. *Microstructures* 2022;2:2022011. https://dx.doi.org/10.20517/microstructures.2022.02

Received: 10 Feb 2022 **First Decision:** 10 Mar 2022 **Revised:** 18 Mar 2022 **Accepted:** 24 Mar 2022 **Published:** 20 Apr 2022

Academic Editor: Zibin Chen **Copy Editor:** Jia-Xin Zhang **Production Editor:** Jia-Xin Zhang

Abstract

Two-dimensional (2D) magnets have evoked tremendous interest within the research community due to their fascinating features and novel mechanisms, as well as their potential applications in magnetic nanodevices. In this review, state-of-the-art research into the exploration of 2D magnets from the perspective of their magnetic interaction and order mechanisms is discussed. The properties of these magnets can be effectively modulated by varying the external parameters, such as the charge carrier doping, thickness effect, pressure and strain. The potential applications of heterostructures of these 2D magnets in terms of the interlayer coupling strength are reviewed, and the challenges and outlook for this field are proposed.

Keywords: Two-dimensional (2D) ferromagnetism, van der Waals (vdW) crystal, magnetic interaction, physical properties

INTRODUCTION

The advancement of science and technology in modern society has a close relationship with the structuring, functionalization and miniaturization of electronic devices and their immanent components[1,2]. However, for many reasons, such as the limitation of quantum size effects on the traditional Moore's law, it is

necessary to re-examine and understand the different physical behavior of many materials in low dimensions. Exactly, with regards to metallic[3,4], insulating[5-7], semiconducting[8,9], magnetic[10,11] and topological properties[12], materials in reduced dimensions may have different behaviors from their corresponding bulk forms. Furthermore, the scope of related phenomena in these systems is also expanding, including superconductivity[13], multiferroicity[14], charge density waves[15,16], Mott insulators[17], weak localization[18], antilocalization[19], and the Dzyaloshinsky-Moriya interaction[20]. Nowadays, the research of numerous phenomena should be well accompanied by the crossover of research content in many fields.

As shown in Figure 1, among low-dimensional systems, freestanding two-dimensional (2D) materials possess weak van der Waals (vdW) interlayer interactions between adjacent planes, thereby representing an appealing prospect for studying the interplay between various versatile electronic and magnetic phenomena[2,21-25]. In particular, ferromagnetic (FM) 2D materials show strong interplay with orbit and spin moments of different electrons, which are of interest for applications[26,27] such as electronics[28], optoelectronics[29,30], MOKE technology[31], sensors[32], modern communication devices, data storage[33] and energy conversion[34,35]. In addition, for the key role in the theory of magnetism and quantum mechanics, they have shown the possibility of facilitating the study of spintronics and emerging heterostructures combining several novel physical properties together, such as spin-injection[36,37], spin-diffusion[38], spin-filtering[39,40], spin-orbit torque[41], Andreev reflection[42] and 2D hybrid magnetic phenomena[43]. Therefore, realizing a reliable long-range magnetic order in low-dimensional systems at ambient temperature has been an important pursuit for several decades, with numerous attempts from both theoretical and experimental perspectives[44,45].

However, for a long period, the thermal fluctuation was expected to destroy the intrinsic ferromagnetism in low-dimensional systems[46]. In particular, with respect to the calculated quantum spin-*S* Heisenberg model in the Mermin-Wagner theorem, any isotropic and finite-range exchange in low-dimensional lattices at non-zero temperature was proved not to be ferro- or antiferromagnetic (AFM)[47]. On the contrary, the existence of quasi-2D magnetism was widely discussed and examined in the 1960s, showing the stronger intralayer magnetic order residing in planes of the 3D crystals[48]. Later, the advances in ultrathin transition metal film growth facilitated the spawn of atomically thin magnets and directly certified Onsager's assumption of 2D monolayer magnets for the first time[49]. Since the first exfoliation of graphene in 2004[1], a series of 2D materials have begun to be isolated, including hexagonal BN (*h*-BN)[50], black phosphorus[51], MXenes[52], and transition metal dichalcogenides[53] and trihalides[26]. Nowadays, the corresponding theory, production, identification, manipulation, and application of these 2D FM materials have been rapidly expanded and further developed. Intrinsic long-range FM order has been observed in 2D doped graphene[54], Chromium germanium telluride ($Cr_2Ge_2Te_6$)[10], NPS_3 (N = Mn, Fe or Ni)[55-57], CrX_3 (X = Cl, Br or I)[58-61], AY_2 (A = V, W or Mo; Y = S and Se)[62-69], $Cr_2Z_2Te_6$ (Z = Si or Ge)[10,57,70], Fe_3GeTe_2[44,71,72] and $MnBi_{2n}Te_{3n+1}$ (n = 1, 2 or 3)[12,73], meaning that this long-debated issue has resulted in a positive consequence. These developments are particularly important for the research into promoting the correlation and functionalization of multiple physical phenomena, and there is a need for more reviews to integrate them.

In this review, we first provide a brief introduction to the mechanism of 2D magnets, their fabrication techniques, the origin of their magnetic interactions, and the manipulation of their low-dimensional magnetism. We then review several typical 2D ferromagnet families that have been realized experimentally and widely studied in recent years. For each family, we first introduce their crystal structure and extrinsic physical properties and then analyze their intrinsic magnetic interactions, mechanisms, and potential applications. We finally conclude with a general outlook regarding future opportunities and challenges.

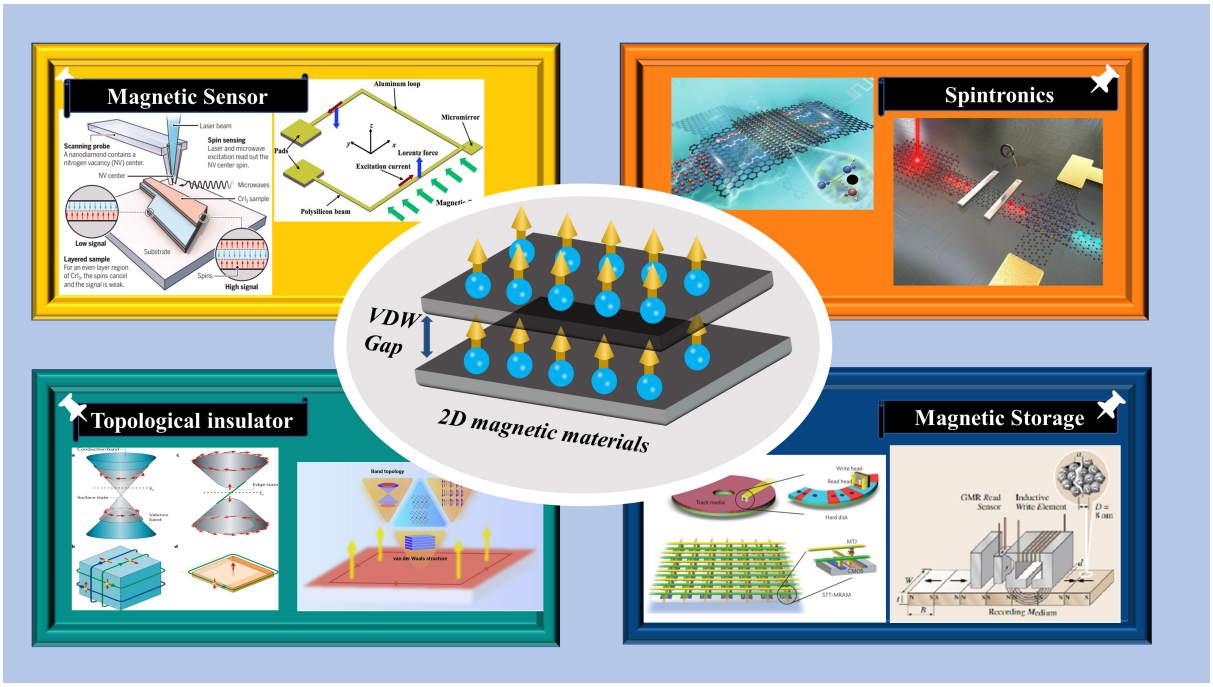

Figure 1. Experimentally verified intrinsically magnetic 2D materials and their potential applications in magnetic sensors[22], spintronics[23], topological insulators[24] and magnetic storage[25].

FUNDAMENTALS OF 2D MAGNETISM AND 2D VAN DER WAALS MAGNETS

Categories and synthesis of 2D van der Waals magnets

Generally, most magnet moments in 2D magnets originate from the orbital and spin angular momenta of the 3*d* or 4*f* electrons in the transition metals, and often interact with their periodic symmetric structures such as crystal field[74]. Based on their crystalline period symmetries shown in Figure 2, the classification of the discovered 2D magnets can be mainly divided into hexagonal, triangular, tetragonal, and orthorhombic lattices[75]. The first group is the layered transition metal hexagonal lattices, which include binary transition metal trihalides MX_3 (M = Cr, V or Ni; X is a trihalide)[8,58,59], NPS_3[76,77] (N = Mn, Fe or Ni) and $Cr_2Z_2Te_6$[78] (Z = Si or Ge). Second, the structure of Fe_3GeTe_2[79], $MnBi_{2n}Te_{3n+1}$[73,80], and prismatic (2H) or octahedral (1T) binary transition metal dichalcogenides such as AY_2 (A = V, W or Mo; Y = S and Se)[53,62,81]are classed as triangular lattice magnets. Third, square and rectangular lattices are also potential 2D magnets and include binary tetragonal iron monochalcogenides, trinary orthorhombic transition metal hetero-anionic halogenide chalcogenides, and trinary orthorhombic vanadium oxide bi-halogenides[75]. Most of the currently known 2D FM materials can be classified using the above systems.

Owing to the fabrication of monolayer or few-layer magnetic crystals mainly referring to their crystal type and phase diagrams[71], the selection of an effective synthesis method is a prerequisite for realizing high-crystallinity, high-quality, low- or non-defective, and ambient stable 2D magnets with controllable atomic thickness. The popular chemical vapor transport method is an effective and reliable technique that can crystallize macroscale high-crystallinity layered magnets, including MPS_3[82], CrX_3[59], VSe_2[3], $Cr_2Ge_2Te_6$[78], and Fe_3GeTe_2[83], where transport agent and temperature zone control have significant impacts on the synthesis. Moreover, sublimation techniques have proved to be useful, direct, and low-cost self-transport methods that have been used to grow transition metal halides. Based on phase diagrams, a flux zone growth method, with the solution phase spontaneously nucleating and crystallizing, which requires high solubility, low competing phases, and the removal of exceeding flux, has been applied to achieve large and high-

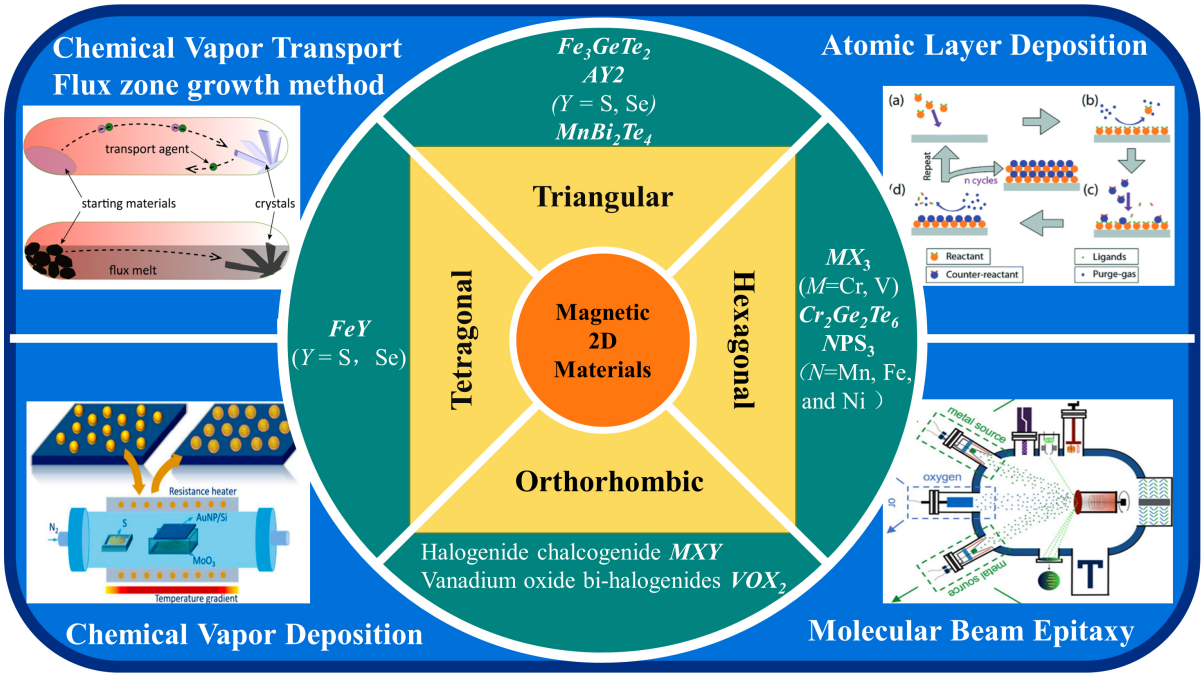

Figure 2. Classification of crystal structures of 2D ferromagnets and their popular synthesis routes, including chemical vapor transport[83], flux melting[84], atomic layer deposition[86], chemical vapor deposition[85] and molecular beam epitaxy[87].

crystallinity 2D magnets[84]. Specifically, the synthesis strategy relies on the characteristics of the material and its environmental demands. Generally, the above-mentioned products synthesized by the top-bottom strategy always require extra isolation, such as the use of Scotch tape, substrate-assisted exfoliation, and liquid exfoliation to obtain atomically thin films.

In contrast, bottom-top thin film synthesis can be a promising option, with chemical and physical vapor deposition[85], atomic layer deposition[86], molecular beam epitaxy (MBE)[87], magnetron sputtering and thermal evaporation having been successful. These space-confined growth methods provide good thickness control to enable the fabricating restriction at a low crystallization speed via *in-situ* nucleation and growth dynamics. Among them, the chemical vapor transport and physical vapor deposition methods have been widely dedicated to the fabrication of various 2D magnets, including VSe_2[64], VTe_2[88], and CrI_3[89]. The precursors directly react without additional reagents, and the thickness and size of the crystals show a strong relationship with time, temperature, carrier gas type, and flow rate[90]. Another advanced approach producing high quality 2D magnets is the MBE technique, which is usually attached to characterization facilities, such as electron diffraction (ED), scanning tunneling microscopy (STM), angle-resolved photoemission spectroscopy (ARPES), *etc.*, and thereby realize the in-situ characterization of the properties for the as-synthesized materials[64,91].

Some novel 2D magnets are expected to be fabricated by adjusting the relevant synthesis parameters, such as reaction temperatures, substrate types, and dopants. In particular, when the total energy of the system restricts the crystal structural stability limit, the self-limited epitaxial growth can be used to directly obtain atomically thin films by challenging the intrinsic isotropic chemical environments and the unpaired dangling bonds at the vdW surfaces. This can effectively extend the synthesis scope of vdW layered materials for producing 2D ferromagnets[92]. The theoretical and experimental study of the atomic

distribution, time and spatial symmetry, and the atomic bonding features at crystal and vdW surfaces has a significant impact on the controllable fabrication of 2D magnets and has accelerated the design of novel and stable high-temperature 2D ferromagnets[9]. Under the guidance of these methods and theories, 2D magnetic materials systems are currently rapidly expanding.

Theory of 2D magnetism

Among the effective interactions for neighboring spins, the indication of forming magnetic order lies in the magnetic moments aligning to a certain direction with the spontaneous breaking of the time-reversal symmetry (TRS)[93]. This long-range arrangement is dominated by several general parameters and tends to be violated by the fluctuations at finite temperature (critical temperature), particularly the dimension factor in critical behavior[94]. For low-dimensional magnets, the long-range ordered spin waves or magnons in this Goldstone mode can be destroyed by thermal fluctuations at low-energy excitations, particularly for 2D systems with more complex competitive relationships. The case of a gapless collective excitation, known as Goldstone modes[71], is often associated with the broken TRS phase and is widely discussed in the contexts of Landau-Peierls instability[71], Hohenberg superconductors and superfluids[46] and the Mermin-Wagner theorem[47]. For this description, the survival of long-range order at finite temperature basically depends on the level of phonon excitation and the spin dimensionality, thereby determining the critical magnetic characteristics of the system, such as the transition temperature and magnetic anisotropy, as shown in Figure 3A[95].

In view of spin-wave theory, the Mermin-Wagner-Hohenberg theorem claims that the gapless long-wavelength excitation can be easily excited at any non-zero temperature that would destroy the long-range ferro- and antiferromagnetism in the isotropic Heisenberg model[47]. It is noteworthy that this proof is centered on a discussion regarding exchange interactions at finite temperature based on isotropic Heisenberg models that theoretically rule out the existence of intrinsic long-range crystalline and magnetic order in 2D and 1D systems. In other words, it does not preclude the magnetic order in situations where the spin dimensionality n is less than 3 or the possibility of stable magnetism by introducing external factors and intrinsic anisotropy[96]. Consequently, the introduction of anisotropy (low spin dimension) may be applicable for protecting magnetism in low-dimensional systems. Therefore, according to relativistic effects, long-range magnetism in low-dimensional systems can be achieved by breaking the spin symmetry by introducing magnetic anisotropy. For example, for the spin dimensionality of 3 in Figure 3B, the isotropic Heisenberg model (n = 3) is absent of magnetic anisotropy, while the Ising model (n = 1) and XY (n = 2) circumstances enable strong easy-axis and easy-plane anisotropy at a non-zero temperature[94]. Generally, for most magnetic insulators and conductors, simplifying a spin Hamiltonian is appropriate to discuss the magnetic properties to some extent. This description mainly contains four factors, namely, exchange (Heisenberg) interactions, anisotropic exchange, single-ion anisotropy, and the introduction of an external magnetic field. However, in specific situations, additional terms, such as Kitaev interactions[97,98], biquadratic exchange[99], Dzyaloshinsky-Moriya interactions[100,101], dipolar interactions[102], interlayer interactions[103] and surface magnetic anisotropy[96], should also be considered, which may also contribute to anisotropy.

To better understand this complex, competitive behavior, the presence of magnetic interactions must be introduced, as described in Figure 3C[95]. First, for the exchange interaction, the primary origin of this magnetic interaction lies in the effectiveness of the interaction, including the direct exchange amid neighboring spins and indirect exchange mediated by the intermediate states of the atoms. Herein, the direct exchange is heavily localized spatially, and indirect exchange is delicate to the energy difference and hopping energy of the intermediate state. The change in band energy by thickness modulation is responsible for the evolution of indirect exchange. Next, a source of anisotropic exchange derives from the two localized spins of bonding element and is mainly determined by spin-orbit coupling (SOC). With the SOC

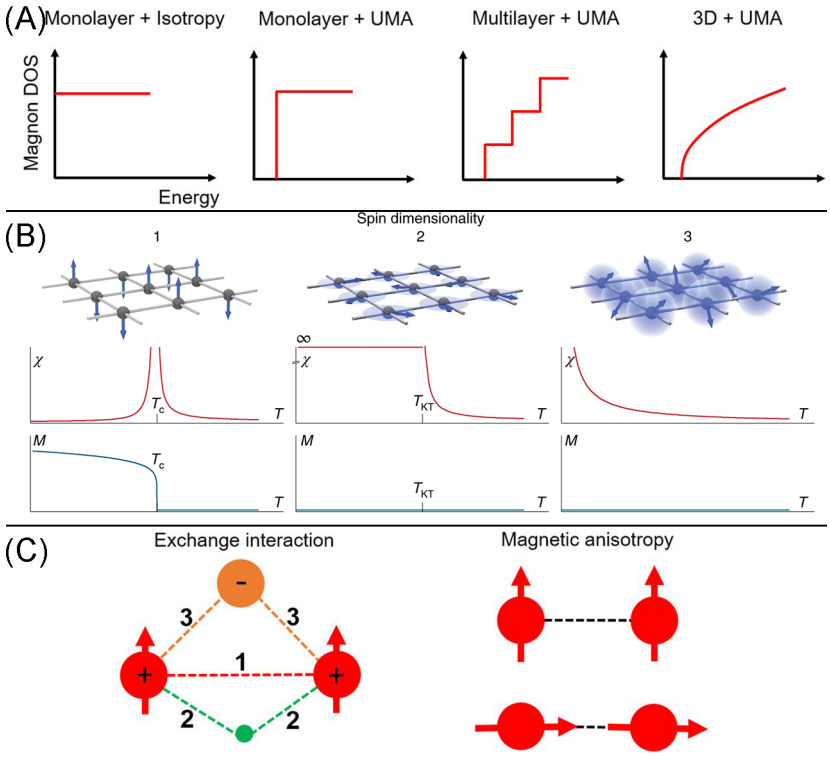

Figure 3. (A) Magnon DOS variation with the system evolving from 2D isotropic to 3D and from isotropic to uniaxial magnetic anisotropy[95]. (B) Schematic of spin orientation and critical temperature change with evolving spin dimensionality, where n = 1 correlates to the Ising Hamiltonian with strong uniaxial anisotropy and n = 2 and n = 3 correspond to an easy-plane anisotropy (XY Hamiltonian) and isotropic Heisenberg Hamiltonian, respectively[94]. (C) Exchange interaction modes and preferred magnetic orientation showing diverse magnetic anisotropy[95].

interaction, the crystal field breaks the degeneration orbital that could produce the unquenched orbital moments, resulting in magnetic anisotropy. Generally, the ligand anion generates large SOC that assists anisotropic exchange, and the SOC in the transition metal contributes to the magneto-crystalline anisotropy, as well as the orbital magnetic moment[58]. Another case of easy-plane magnetocrystalline anisotropy mainly takes place in dipolar interaction Heisenberg magnets[102] with a Kosterlitz-Thouless phase transition. Another case is the single-ion anisotropy from the interplay between the local crystal field and SOC, where its Hamiltonian depends on the high-spin state of the ion from the perturbation theory. With degeneracy, this anisotropy belongs to the first-order perturbation, whereas the second-order perturbation is another case of anisotropy without degeneracy[71]. For example, for transition metals with a well-defined symmetric crystal field, the single-ion anisotropy is regarded to be stable, and this situation can be modulated by the Jahn-Teller effect in the octahedral structure. In short, magnetic interactions are an important origin of magnetic anisotropy and provide the main contribution to magnetism.

Magnetic states belong to an exhibition of the macroscopic features of ferromagnetic behavior from these interactions. First, as described above, the macroscopic magnetic characteristics are mainly attributed to the interactions between the local spin or the itinerant ferromagnetism of magnetic ions, including interlayer and intralayer accumulations/competitions. As shown in Figure 4, an FM state shows all spins in the lattice arranged in the same direction, while AFM states represent zero net moments where neighboring spins usually align in opposite directions on different sublattices. The magnetic state and order have a close relationship with the lattice parameters. Second, the magnetic anisotropy energy (MAE) represents the

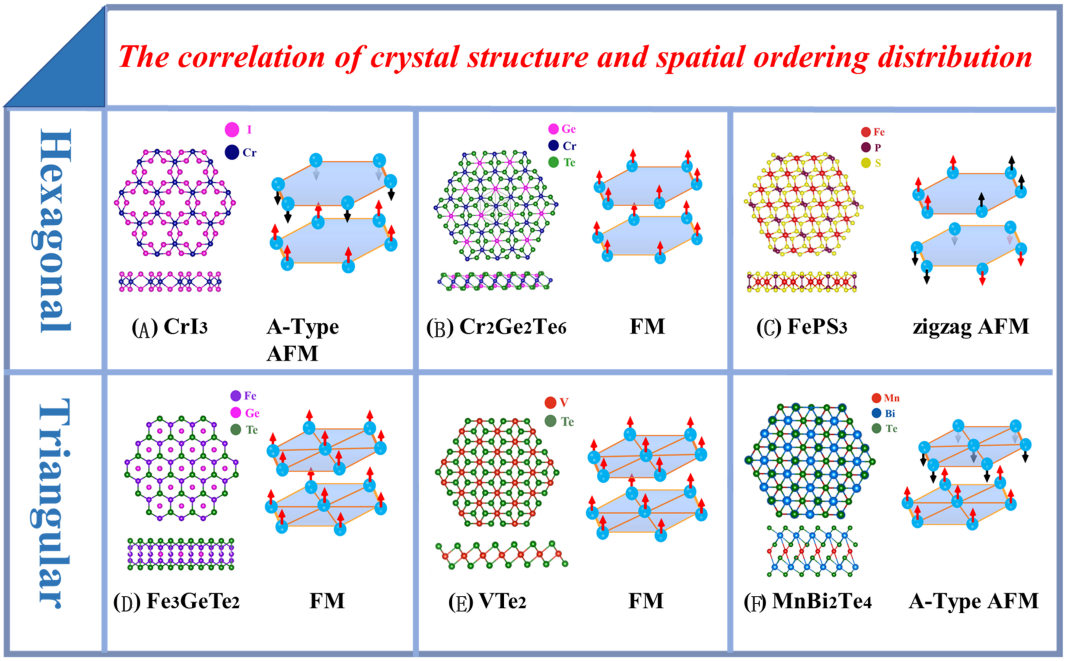

Figure 4. Correlation of crystal structure and the corresponding spatial ordering distribution for each material family, including hexagonal (A) CrX_3, (B) $Cr_2Ge_2Te_6$ and (C) NPS_3 and triangular (D) Fe_3GeTe_2, (E) AY_2 and (F) $MnBi_{2n}Te_{3n+1}$.

energy difference from the magnetic easy axis to the hard axis, showing the degree of stability of the long-range spin order in 2D materials. According to the magnetic moment arrangement orientations, they are classified as Heisenberg-, XY- and Ising-type magnets and are dominated by the interaction between the magnetic moments and the crystal field. Third, numerous internal or external conditions, including fields, fluctuations, and interactions, exhibit fierce competition at different temperatures or magnetic fields, leading to complex moments and multiple critical points that describe the critical magnetic phase transition behavior in 2D magnets. This evolutionary process is appealing for studying the interplay among 2D magnets.

Theoretical modeling is a powerful tool for predicting possible ferromagnets with the desired magnetic behaviors. For example, the group of Kan proposed several approval solutions by calculation predictions. The first step was to determine a certain magnetic semiconductor element A in the transition metal region, followed by a selection of another element B that should meet the same occupation state as A when embedded in the basis. Finally, the energy gap opened by the crystal field between A and B should be considerable[9,104]. Furthermore, the spin-polarized materials only with *s* or *p* orbital hybridization should meet the coexistent demand of super-exchange and carrier-mediated interactions. This proposal also effectively promoted the research into the design of advanced ferromagnets.

The development of 2D magnets remains a work in progress, and the origin of the interactions and magnetic behavior at the 2D limit requires further study. In particular, a simplified model to describe the complex mechanism of interactions and the ability to predict novel 2D ferromagnets with good magnetic performance is required. These factors could help us to design and synthesize an ideal 2D vdW ferromagnet with robust magnetic behavior and high stability, thereby promoting the research into condensed physical properties.

Emergent physical properties and tunable ferromagnetism

In addition to ferromagnetism, other exceptional physical properties and their interactions with magnetism have also motivated many studies and potential applications. In Figure 5A, many fascinating magnetic properties can be explored in intrinsic 2D magnets[105]. For example, considering the band energy in vdW materials, achieving the combination of ferromagnetic and semiconductor properties in ultrathin films has realized the long-term desire of spintronics. In contrast, atomically thick ferromagnetic half-metals and metals are also good choices for emerging robust spin orders, such as high critical temperatures[4] and spin polarization ratios[38]. Furthermore, many interesting topological quantum phenomena can be reached by controlling the spin parameters in 2D ferro- and antiferromagnets, such as axion and Chen insulator behavior with quantum anomalous Hall effects, as shown in Figure 5B[106]. Magnons can represent a collective behavior of magnetic moments that can be basically regarded as a quantized spin wave and obey Bose-Einstein condensation[107]. Therefore, they can associate spin states with magnon behavior in 2D vdW magnets. Dzyaloshinskii-Moriya interactions can stabilize topological spin textures known as skyrmions in 2D vdW magnets and have promising potential in spintronics technology, such as low-energy-consumption logic and memory devices[108-110]. To describe the relaxation degree to the equilibrium constant value of magnetization in a 2D magnetic single crystal, which is mainly affected by the SOC band structure and electron scattering, the parameter of anisotropic Gilbert damping determines the performance of many spintronic devices[111].

Furthermore, the interactions between intrinsic magnetism and other physical quantities can produce numerous meaningful applications and novel phenomena. For instance, first, the behavior of magnetization and specific heat belongs to magnetocaloric effects, and the application of magnetic refrigeration can obtain ultralow temperatures. Second, in view of magneto-optic effects, one method is to measure the light reflection or transmission, including the Kerr, Faraday, and Cotton-Mouton effects, magnetic circular birefringence, and dichroism, while the other is to analyze the effect of light on the materials before and after the interaction with photons, as shown in Figure 5C and D[112]. Polarization-resolved photoluminescence measurements represent a powerful technique for probing magnetism[113], particularly for identifying the coupled valley pseudospin in valley physics by constructing heterostructures[114]. Third, inspecting the interplay of spin-phonon coupling via inelastic light scattering from optical phonons is ideal for studying phonon performance[115]. Fourth, another phenomenon related to magnetism and transport properties, including the measurement of lateral and longitudinal resistance, reveals the critical physical property of the spin-order effect on the electron scattering and potential charge density wave transitions. Furthermore, some indirect relationship between electric phenomena and magnetism could be used to investigate valley and spin splitting[114]. Moreover, the effective interactions between magnetization and electric polarization bring about multiferroic behavior, which is promising in the practice of spintronics and microwave magneto-electrics. In addition, the research of interplay on the magnetic and superconducting fluctuations with van Hove singularities in the electronic spectrum enables us to further investigate the quantum-critical behaviors in 2D systems[116]

Eventually, by understanding the above-mentioned physical properties in 2D vdW magnetic materials, the design and control of magnetism become optional and operative. First, the size and edge effect on the band structure suggests the existence of edge magnetism from a series of theoretical calculations[117]. Second, the introduction of defects, including holes, impurities, dislocations, and domains, can effectively modulate the density of states of electrons in crystal lattices, thereby affecting the chemical environment and changing the magnetic order behavior. In particular, the proximity effect can drive various interesting physical properties by constructing asymmetric structures with two distinct surfaces in 2D magnets, including forming multiferroicity and ferroelasticity in 2D Janus magnets and superconductivity, frustrated magnetism and anisotropic spin texture through the adjacent regions in 2D heterostructures[45,118]. Third, electric fields and

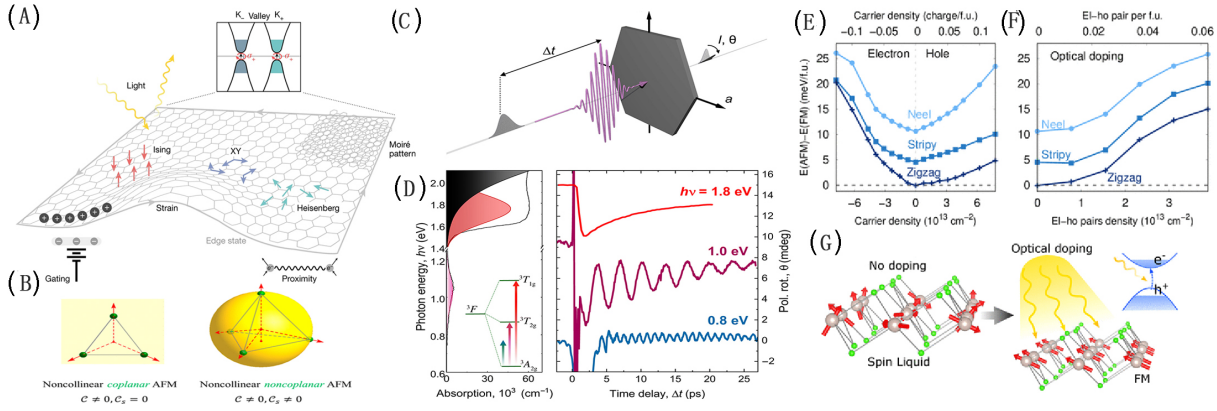

Figure 5. (A) Physical phenomena that can be studied with magnetic vdW materials[105]. (B) Schematic of spin-orientation-dependent QAH and QSH effect associated with different AFM states[106]. (C, D) Dynamics of time-resolved pump probing, phonon energy and delaying time spectra of $NiPS_3$ [112]. (E, F) Energy differences of AFM phase by unipolar doping and optical electron-hole doping. (G) Tunable 2D magnetism by optical doping of monolayer $RuCl_3$ [120].

external strain on the lattice usually influence the interactions among ions and tune the electronic band structures, hence changing the magnetic states, insulting states, critical points, and various other physical quantities[119]. Finally, phase transitions can also be induced by free carriers and can produce electron-hole pairs by light, as shown in Figure 5E-G, and therefore form a proximate spin liquid, enabling a new tool to construct 2D magnetism[120]. To summarize, regardless of the progress that has been made for emerging multiple physical behaviors, many of them are anticipated to be modified and further verified in the future.

LONG-RANGE MAGNETISM IN VAN DER WAALS MATERIAL FAMILIES AND THEIR APPLICATION ADVANCES

In the previous section, we briefly discussed the synthesis methods and mechanisms in magnetic interactions, magnetism with other physical properties of 2D magnetic materials, as well as their interaction and regulation approaches. In this section, based on their relevant structural and magnetic properties, we specifically present several vdW FM material categories that have been experimentally synthesized and manipulated recently in detail. Beginning with each family, we start with a brief introduction of their lattice distribution features and characteristic magnetic behaviors and analyze their physical properties and manipulation methods. We then discuss their detailed magnetic features, including possible exchange interaction coupling, coupling magnetic anisotropy, intralayer and interlayer exchanges, potential electron/phonon/magnon coupling, magnetic domains, and critical behavior. Next, we summarize the highlights and open questions based on the research status of each family. Finally, by combining the introduced families, we concisely review the advances in heterostructure applications and their modulated physical phenomena.

Binary transition metal chromium trihalide family (CrX_3, X = Cl, Br, or I)

Theoretical and experimental studies indicate that exfoliated transition metal trihalides MX_3 (M = Cr, V or Ru; X = Cl, Br or I) have very interesting electronic and magnetic properties, including chromium trihalides CrX_3, the ferromagnet vanadium triiodide VI_3 [121] and ruthenium trihalides RuX_3 [122]. Due to their interesting topological and spintronic properties, these metal halides have received significant attention[27]. For these chromium trihalides, they possess extinct magnetic diversity but share a common honeycomb iso-structure, with the edge-sharing octahedra formed by six halide anions at the corners and a trivalent chromium cation at the center. Calculations have shown that the localized d-orbital electrons in Cr^{3+} and the weak dielectric screening in the vdW structure can produce a large bandgap around the Fermi level, indicating that the CrX

$_3$ family behaves like an insulator[93].

Distinct differences in the cleavage energy and stiffness between the in-plane and out-of-plane structures enable a facile exfoliation of a few layered chromium trihalides, including $CrCl_3$, $CrBr_3$, and CrI_3. All three chromium trihalides are found to exhibit a strong intralayer FM coupling and multiple magnetic phases, as shown in Figure 6A, but these compounds hold three different magnetic behaviors[123]. Firstly, $CrBr_3$ is a ferromagnet in both bulk and monolayer forms, with a layer-dependent T_c of 20-37 K, where the magnetic anisotropy easy axis is vertical to the vdW facet[124]. Simultaneously, the CrI_3 ferromagnet displays a similar out-of-plane easy axis with the T_c ranging from 45 to 61 K from a single layer to a multilayer[58]. It is also noteworthy that CrI_3 exhibits a ground state of AFM coupling when stacking over two layers, as well as an interesting layer-by-layer spin-flip transition at ~0.7 T[94]. In contrast to the Ising model described for $CrBr_3$ [125] and CrI_3[61], bilayer $CrCl_3$ can persist with an XY model form of easy-plane anisotropy interlayer AFM resonance, with a thickness-independent T_N of ~16.8 K[84], which could facilitate research into topological vortices and the potential Berezinskii-Kosterlitz-Thouless (BKT) transition in this system. The substitution of halogen elements in the same main group has led to drastic changes in the magnetic behavior, indicating a series of mechanisms to be discovered and explained.

Considering the intralayer exchange in CrX_3 monolayers, the spin-spin interaction is mainly predicted by two interactions, as shown in Figure 6B-E[126]. One is an AFM interaction formed by the nearest neighboring direct exchange interaction via the nearest Cr-Cr neighbor[125]. The other is an FM form introduced by the next-nearest neighboring halide-mediated super-exchange pathway via the half-filled *d*-orbital t_{2g} of the Cr atom and empty *p*-orbital e_g of the halide ions. With the metallicity and atom radius increasing from Cl to I, the covalency of Cr-X can be strengthened and the distance of Cr-Cr is enlarged, resulting in a more powerful Cr-X-Cr super-exchange interaction and a weakened Cr-Cr direct exchange interaction[127]. Furthermore, in the case of CrI_3 and $CrBr_3$, shown in Figure 6B, the heavier halide atoms lead to a stronger spin-orbit interaction to stabilize ferromagnetism within the intralayer. Therefore, a tendency of intralayer AFM-FM-AFM by the occupation from Cl to I can be explained by the synergy effect of the spin-orbit interaction and the competition between the nearest and second nearest neighbors. Interestingly, due to the lack of effective approaches that could obtain and then character monolayer magnetism in $CrCl_3$. The issue of the easy-plane magnetism in monolayer $CrCl_3$ was verified to be intralayer ferromagnetic until X-ray magnetic circular dichroism (XMCD) evidence of an MBE grown monolayer $CrCl_3$ in 2021[128], thereby enriching the physics and universality scaling of phase transitions in low-dimensional systems.

Generally, the interlayer exchange interaction in few layers can be promoted to their bulk forms. However, the circumstances in CrI_3 and $CrCl_3$ are not as generally expected. Noting there are two stacking configurations of monoclinic (antiferromagnetic t_{2g}-t_{2g} dominated) and rhombohedral (ferromagnetic t_{2g}-e_g dominated) in CrX_3, possible speculation of the phase transition may occur not only with the temperature change, but also with the thickness accumulation. It is noteworthy that, by means of theoretical calculation[103] and experimental results[129], a thickness-dependent phase transition of monoclinic to rhombohedral at low temperature can exist in the CrI_3 system. Therefore, this emphasizes the importance of the stacking form for the regulation of ferromagnetism/antiferromagnetism. In addition, Figure 6F-Hshow a linear spin-wave for the magnon dispersion that has shown that a topological origin of the opened Dirac gap at the Γ-point stabilizes the magnetism[17], due to the existence of both the single-ion uniaxial anisotropy and super-exchange interaction mechanism in the off-plane $CrBr_3$ and CrI_3. According to the Ising model, magnetic order is destroyed by spin-wave proliferation; therefore, the Curie temperature of $CrBr_3$ and CrI_3 is dominated by spin-wave proliferation[130].

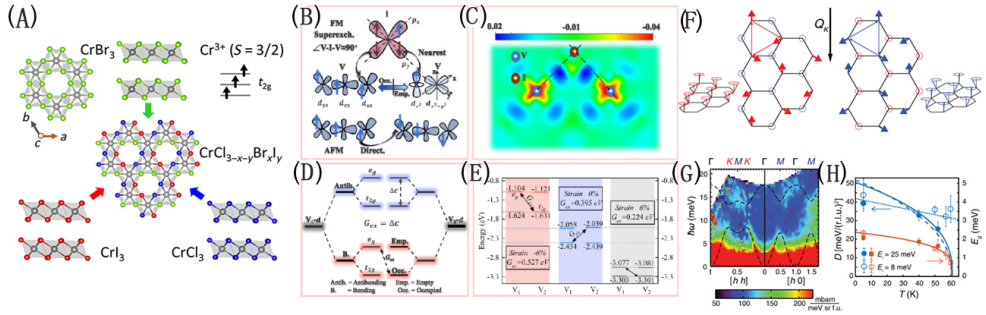

Figure 6. (A) Structures of vdW CrX_3 [123]. (B) Schematic diagram of super-exchange and direct exchange. (C) Spin displacement of two sublattice spins at the right-handed chiral wave in CrI_3. (D) spin-wave excitations at T = 52 K and (E) temperature dependencies of the stiffness of the acoustic mode of CrI_3 [126]. (F) 2D charge density difference for a certain plane. (G) Schematic diagram of exchange mechanism and d-orbit energy level splitting of V-V bonding. (H) On-site energies for *d* orbitals of nearest-neighbor V atoms with different strains in monolayer VICl[17].

Although numerous studies have attempted to explain the interplay in the vdW ferromagnet CrX_3, the genuine origin of the inter- and intra-layer Heisenberg exchange interaction needs to be given further attention in consideration of the detailed evolution of the extra exchange interactions, orbital environment, and Coulomb interaction. In addition, the magnetic anisotropy originating from various anisotropy Hamiltonians, such as anisotropic exchange, single-ion anisotropy, Kitaev exchange and the Dzyaloshinsky-Moriya interaction, should be further valued, especially the topologically protected item[131].

Despite the tunable magnetism in the CrX_3 family, the application of vdW ferromagnets is still far from the requirement of maintaining a stable FM spin array that could survive over ambient temperature. A series of strategies for constructing novel geometries of atoms and modulating different electronic interactions have been applied to change the magnetic behavior in 2D materials. For example, as mentioned above, consideration of changing the bond angle and length may affect the electronic structure and magnetic behavior. A delicate design of mirror symmetry (out-of-plane) violation by constructing a Janus Y-C-X heterostructure (where C is generally a transition metal and X and Y are two different halide or chalcogenide elements) can effectively adjust the intrinsic and extrinsic behaviors, such as semiconducting[115] and metallic/half-metallic behavior[43,132], spin and valley polarization[133,134], magnetic anisotropy[135,136], robust ferromagnetism[137], multiferroicity[138], stabilized spin flips[132] and the Dzyaloshinskii-Moriya interaction[139,140]. Furthermore, more 2D magnetic crystals with a similar structure (such as VBr_3, VI_3, and $NiBr_3$) have been examined and have also attracted much interest because of their tunable magnetism and fascinating SOC behavior[8,141]. By combining these two methods, another study revealed an enhanced T_c of 240 K for vanadium trihalides by creating a Janus V-X-Y configuration[126]. As Figure 6H shows, with a 6% tensile strain, the T_c in this structure can be further promoted to 280 K, which represents an important step in enriching the family of ambient vdW ferromagnets.

Binary transition metal dichalcogenide family (ASe_2, A = V, Mn or W)

With more advanced approaches achieved in vdW ferromagnets, a variety of materials with a tendency for high T_C, as well as more accurate property detections, have emerged. In turn, the in-depth physics around the magnetoelectric interaction has been inspired. For example, layered vdW materials have shown a significant variation of characteristics when they have been thinned to a monolayer, including transitions between indirect and direct bandgap materials[16], many-body quantum criticalities[13] and field tunable properties of many-body states, as highlighted in Figure 7A[42].

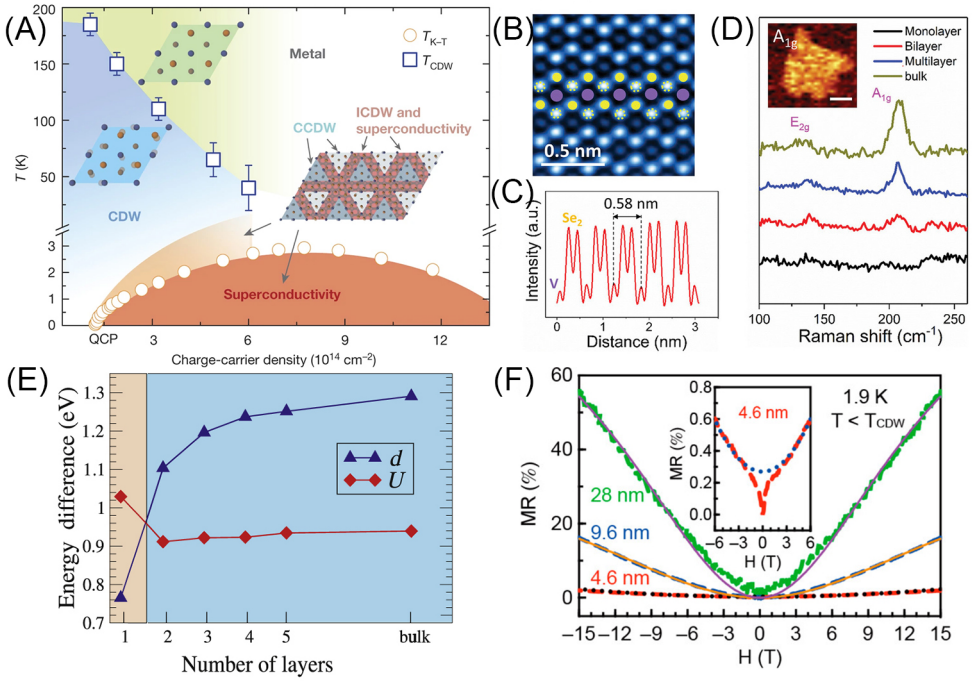

Figure 7. (A) Phase diagram and physical properties of $TiSe_2$ under electron doping[42]. (B) Atomic-resolution STEM image and (C) intensity line profile of exfoliated VSe_2 flake and (D) layer-dependent Raman spectra (inset: mapping) of VSe_2 from monolayer to bulk[143]. (E) Metal-insulator phase transition schematic of VSe_2[149]. (F) Magnetoresistance of VSe_2 nanosheets with different thicknesses, showing WAL effect features by HLN fitting[19].

As a versatile family of 2D materials, pristine 2D transition metal dichalcogenides possess trigonal 2H or 1T structures with potential features such as semiconducting[142], metallic[143] and charge density wave (CDW) behavior[144]. Among them, VSe_2 is a six-fold symmetric hexagonal structure with the V atom located in the middle layer, separating two layers of Se atoms. XMCD results confirmed ferromagnetism in a 1T-VSe_2 monolayer flake at a T_c of 470 K, with a magnetic moment of 0.3 μ_B per V atom. From Figure 7B-D, for the vibration signals of VSe_2 in Raman spectra, when reducing the bulk thickness to a bilayer, the intensity ratio of the two peaks of E_{2g} (in-plane) and A_{1g} (out-of-plane) changes dramatically[143]. When combined with the broadened XRD peaks of exfoliated VSe_2 nanosheets, the results suggest a highly crystalline c-axis orientation in the exfoliated VSe_2 nanosheets. With no evident shift or splitting for the 3*d* orbital of Se and the 2*p* orbital of V in the XPS peaks found in few-layer VSe_2 before and after the exposure to air, its air stability was further evidenced[145].

Interestingly, experimental results exhibit paramagnetic characteristics in bulk VSe_2, whereas it can behave as a ferromagnet when thinned to a monolayer[18], i.e., spontaneous magnetization exists in 2D VSe_2 rather than in 3D. An explanation of this phenomenon should be noted by the density of states (DOS) at the Fermi level (E_F) being greatly enhanced when tunning the critical thickness of VSe_2 to a bi- or monolayer[146]. The Stoner criterion can be enhanced when the density difference of electrons between the spin-up and spin-down states is enlarged. Similar behavior was found in $NbSe_2$[62], $PtSe_2$[147] and $MoSe_2$[148]. Furthermore, theoretical work has also predicted a metal-insulator transition, as shown in Figure 7E[149], and a huge discrepancy in saturation magnetization with different substrates for the epitaxy of monolayer VSe_2. As Figure 7E shows, with the layer number increasing, the intraband coupling of the d value (blue line) ascends while the Coulomb energy of the U value (Red line) descends, and the competition between these values results in the change of bandgap from indirect to gapless. Furthermore, calculation results have shown that

the SOC effect of monolayer VSe_2 induced a large MAE of ~1.1 meV.

For manipulating ferromagnetism, doping and stress tuning can lead to strong valley splitting by SOC, and structural rearrangement is able to induce a Peierls distortion to open up the energy gap at E_F, thereby frustrating the magnetic moment of the TMD monolayer[15]. For example, results indicated that an Mn dopant reinforces the long-range ferromagnetism in some TMDs, including MoS_2, $MoSe_2$, and $MoTe_2$, which is much stronger than the substitution of Fe, Co, and Ni. The explanation for this lies in the balance of the AFM coupling from the direct exchange of two localized Mn 3*d* states and the FM coupling from the super-exchange of delocalized *p* states of the chalcogen with Mn[150]. Another statement clarified a key factor of the short-range double-exchange mechanism when Mn dopants are inserted at Mo sites that controls the long-range magnetic order[142]. Furthermore, Wang and co-workers demonstrated that a proper substitution at the Mo site at nonmagnetic MoS_2 or Mo vacancies favors the FM coupling, thereby transforming to an intrinsic diluted magnetic state[151]. Furthermore, the tensile-based transport property of TMDs was investigated by DFT, and the results showed an evident difference in the bandgap, effective mass, elastic modulus, and deformation potential by applying tensile strain from different directions[152].

However, doubts regarding whether the magnetism originates from a certain band structure spin splitting remain a controversial issue for the complex bandgap that indicates FM exchange-splitting[75]. For example, on the one hand, due to the possibility of CDW, the phase transition temperature in this system can be suppressed[153]. On the other hand, even though the reduction of the DOS at the Fermi surface would be aroused in the bulk form by changing the CDW, the phase transition temperature would also be lowered when the thickness is reduced[15]. Additional evidence for this is the quasi-2D transport with magnetoresistance and the weak anti-localized (WAL) effect that was clearly observed in heptalayer VSe_2 below 10 K. The WAL results in Figure 7F fit well with the Hikami-Larkin-Nagaoka equation, indicating that the dephasing mechanism is electron-electron interaction dominated[19]. In summary, judging the origin of magnetism in few-layer VSe_2 is a matter that requires attention and is awaiting a series of further experimental results to clarify it.

Ternary transition metal phosphorus trisulfide family (NPS_3, N = Mn, Fe or Ni)

The transition metal phosphorus trisulfide compounds NPS_3 (N = Fe, Mn, or Ni) are a class of vdW stacking AFM insulators (bandgap over 1.0 eV), which can be exfoliated down to the monolayer limit experimentally. These materials serve as good candidates for numerous applications in Li-ion batteries, optoelectronic materials processing, and visible-light water splitting, especially their intriguing magnetic properties. As shown in Figure 8A and B, NPS_3 materials possess a monoclinic $C2/m$ space group that holds the $(P_2S_6)_4$ bipyramidal structure arranged in a triangular form[154,155]. Inside, two-fold symmetry distributed transition metal atoms T are bonded with six S atoms on the upper and lower layers of the T plane with trigonal symmetry, where every six S atoms share a common connection with P atoms[156].

Although these three compounds are isostructural, as shown in Figure 8C, varying the transition metal in NPS_3 results in different AFM orderings due to their different spin dimensionalities, thereby distinguishing the corresponding magnetic states. For $MnPS_3$, the magnetism contains a 3.5 μB interlayer FM ordering along the c-axis with a critical temperature of 78 K, which means the same spin could be reserved in two adjacent layers. In the ab plane, the spin of the two adjacent magnetic ions is reversed, showing Néel-type AFM[76]. According to the crystal field model, the Mn^+ ion is in the high-spin ^6S ground state, and the spin-orbit coupling and triangular distortion of this ground state can be ignored, so the single-ion magnetic anisotropy is small and the magnetic dipolar anisotropy dominates. Therefore, the magnetic susceptibility for $MnPS_3$ is nearly isotropic due to the single-ion and dipolar anisotropy and can be described by the

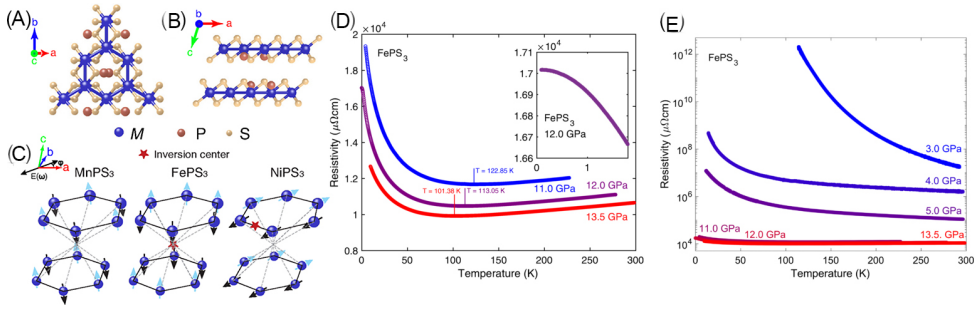

Figure 8. Crystal and magnetic structure of *NPS*$_3$. *NPS*$_3$ lattice viewed along the (A) c-axis and (B) b-axis and (C) AFM structures of *N* PS$_3$[155]. (D) Detailed and (E) whole resistivity survey of FePS$_3$ plotted against temperature at different pressures[160].

Heisenberg Hamiltonian[56].

Interestingly, with the T_N at ~120 K, FePS$_3$ holds another AFM behavior that contains an interlayer AFM coupling and an intralayer zigzag-type AFM coupling, which means the pair of nearest two spins are aligned with the same orientation and opposite to their neighboring pairs. Due to the presence of high spin Fe ions, the triangular distortion and spin-orbit coupling effect are strong, resulting in FePS$_3$ showing a highly anisotropic magnetic susceptibility, which can be well described by the Ising Hamiltonian[56].

For NiPS$_3$ (T_N of ~150 K), different from MnPS$_3$ and FePS$_3$, the spin lies in the ab plane. The interlayer coupling is FM, while the intralayer coupling is a zigzag type similar to FePS$_3$[76]. Its magnetic anisotropy originates from the zero-field splitting of the Ni ion $^3A_{2g}$ ground state caused by a triangular distortion. Since this is an indirect interaction, NiPS$_3$ exhibits weak anisotropy, which can be outlined with the anisotropic Heisenberg model[56]. In summary, due to the diversity of the transition metal, the interaction in the crystal field is different. For NiPS$_3$ and FePS$_3$, the single-ion anisotropy is mainly discussed, while for MnPS$_3$, the magnetic dipolar anisotropy plays a key role.

Recent studies have shown that the magnetic properties of MnPS$_3$ and FePS$_3$ can be maintained in atomically thin monolayers. Using thickness-dependent Raman spectroscopy, Lee and co-workers reported that the Ising-type AFM order of FePS$_3$ persists as the thickness decreases to the 2D limit with almost unchanged transition temperatures[154]. This indicates that the interlayer interaction hardly affects the magnetic ordering of FePS$_3$[154]. Simultaneously, tunneling magnetoresistance measurements performed on MnPS$_3$ show that the magnetoresistance effect always exists with MnPS$_3$ cleaved from the bulk to the monolayer, and even at the monolayer limit, the process from the AFM ordered state to the spin-flop state with an increasing magnetic field can be observed. This suggests that in the MnPS$_3$ system, the antiferromagnetic order can exist in the monolayer and has a magnetic field dependence[157]. This is further demonstrated by an explanation of the broken symmetry of space reversal and time reversal in the Néel ordered state of ultra-thin MnPS$_3$ down to at least 5.3 nm via optical second harmonic generation rotational anisotropy tests.[155] A similar conclusion was found using Raman spectroscopy of MnPS$_3$ from bulk down to the bilayer, showing that as the temperature drops through the Néel temperature, the Raman spectra for the few-layer samples exhibit characteristic changes in the Mn ion vibration-related phonon modes, indicating the surprisingly stable magnetic ordering at a thin limit[82]. For NiPS$_3$, good maintenance of the XY Hamiltonian down to the monolayer limit, its in-plane AFM ordering survival down to bilayer samples and with a slight change of the Néel temperature. However, it is almost completely suppressed when reaching the monolayer limit[77].

In a 2D system, the interaction is very complex but also very interesting. For example, via giant magnetic field magneto-Raman spectroscopy over 30 T, the magnon-phonon coupling can be clearly and directly observed in the 2D AFM semiconductor $FePS_3$. Under the influence of a strong out-of-plane magnetic field, the magnon band observed in the Raman spectrum splits into two sub-bands corresponding to different spins. One of the sub-bands couples with nearby phonons to generate hybridized magnon-phonon quasiparticles. A single-ion magnetostriction-based magnetoelastic Hamiltonian was theoretically established to successfully simulate the experimental results, which clearly confirmed the magnon-phonon strong coupling observed in the 2D inverse model[158]. Simultaneously, extensive spectroscopic measurements and theoretical tools, including spectroscopic ellipsometry, X-ray absorption, photoemission spectroscopy, and DFT calculations, showed that $NiPS_3$ had an abnormal shift in optical spectral weight under the Néel temperature, thereby reflecting the strong charge-spin coupling between the electronic and magnetic structures[159].

We now consider the manipulation of the physical properties in the NPX_3 family[160]. First, an insulator-metal transition was found in $FePS_3$ under high-pressure electrical transmission measurements [Figure 8D], with a significant resistivity reduction occurring when increasing the applied pressure above 3.0 GPa[160]. Furthermore, when the applied pressure reaches 11.0 GPa in Figure 8E, the temperature-dependent resistivity of FPS_3 exhibits an obvious insulator-metal transition, which was further confirmed by high-pressure XRD data. Experiments have shown that the manipulation of pressure in 2D magnetic materials can significantly change the crystal structure and electronic properties. Another advanced technique is using light to control the magnetic anisotropy in $NiPS_3$. Afanasiev and collaborators used ultrashort pulses of light to optically pump $NiPS_3$ on the picosecond time scale[112]. By changing the photon energy during orbital resonance, they could selectively activate the 2D magnon modes at terahertz frequencies, which are controlled by light-induced changes in the magnetic anisotropy axis. The most fundamental principle lies in the change of the magnetic anisotropy axis response to the photoexcitation of ground state electrons to transition to lower symmetry orbitals[112], thereby confirming the control of magnetic anisotropy in 2D vdW AFM $NiPS_3$.

Ternary chromium silicon telluride ($Cr_2Ge_2Te_6$) family

$Cr_2Ge_2Te_6$ is a weak anisotropic ferromagnet semiconductor and possesses an all-direction collective spin moment orientation with a small energy difference below the T_c of 68 K[10]. Along the c-axis of the 2D $Cr_2Ge_2Te_6$, the middle layer of transition metal Cr is sandwiched by two Ge-Te layers, where Te can be replaced by Se and Ge can be substituted by Si and Sn. Based on X-ray and neutron diffraction results, layered $Cr_2Ge_2Te_6$ exhibits a honeycomb structure along the c-axis in Figure 9A, with a vdW distance of 6.9 Å[78]. Raman spectroscopy indicated that each Cr atom possesses a magnetic moment of 2.4 μ_B.

Angle-dependent resistance confirmed that layered $Cr_2Ge_2Te_6$ possesses a uniaxial magnetic anisotropy Heisenberg magnet perpendicular to the isotropic ab-plane[70,161]. Theoretical calculations predicted that the whole magnetic moment is localized at the Cr sites [Figure 9B], thereby leading to long-range ferromagnetism[162]. Its magnetic anisotropic energy is computed to be ~0.1 meV/Cr between the magnetocrystalline and magnetic dipolar anisotropy energies. More critical exponents were fitted and summarized the 2D-Ising ferromagnetism in $Cr_2Ge_2Te_6$ and $Cr_2Si_2Te_6$[163], and more results have shown that the ferromagnetic transition temperature of $Cr_2Ge_2Te_6$ has a relationship with the thickness. Computational results and Kerr rotation experiments have shown the monotonic increment in T_c from bilayer (~30 K) to multilayered bulk (~68 K)[164]. In addition, for bilayer, trilayer, and six-layer samples, applying a slight external field arouses a notable change in T_c[78]. Furthermore, with changing thickness, the electronic structure and magnetic properties of layered $Cr_2Ge_2Te_6$ vary readily, suggesting excellent potential for the construction of 2D vdW devices with facile manipulation.

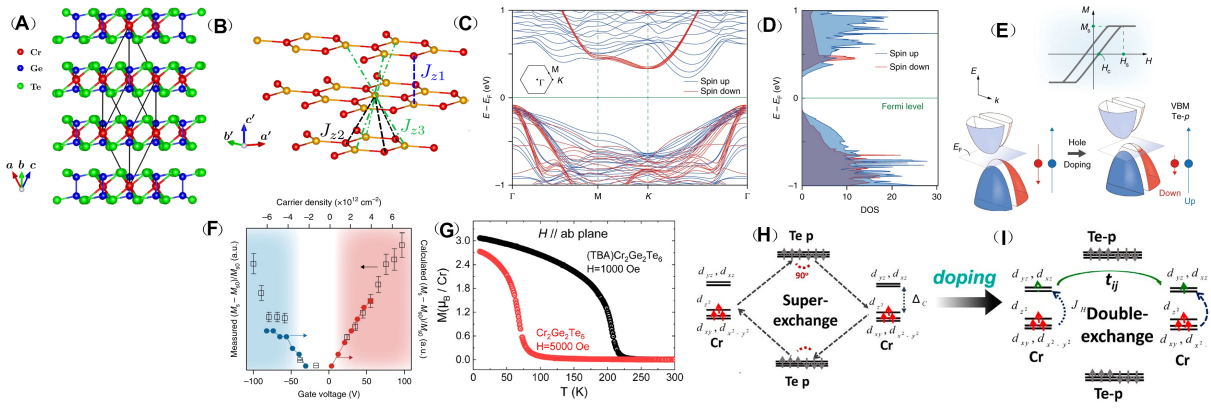

Figure 9. (A) Crystalline structure and (B) exchange coupling figuration of AB-stacked layer of $Cr_2Ge_2Te_6$[78]. (C) Spin-polarized band structure and (D) calculated DOS of few-layered $Cr_2Ge_2Te_6$. (E) Magnetization reversal and spin realignment by carrier doping. (F) Simulated evolution of measured spin magnetization changes by tuning the hole and electron carrier density[153]. (G) Magnetic susceptibility-temperature spectra of organics intercalated $Cr_2Ge_2Te_6$. (H) Comparison of super-exchange interaction in $Cr_2Ge_2Te_6$ and (I) double-exchange interaction in organics intercalated $Cr_2Ge_2Te_6$[168].

Strain and defect engineering are also confirmed to have an impact on the electronic and magnetic characteristics of monolayer $Cr_2Ge_2Te_6$. For example, a semiconductor-to-metal transition in $Cr_2Ge_2Te_6$ can be realized by a compressive isostructural phase transition[165], and an easy-axis direction can be switched by both the effect of Ge vacancies and thickness[166]. Furthermore, for the carrier doping of $Cr_2Ge_2Te_6$, the electric-gate voltage tuning toward magnetization and the magnetic phase transition is found to be sensitive. In particular, the improvement in saturation magnetization can be interpreted by the enhancement of the magnetic moments on Cr atoms. Moreover, as shown in Figure 9C-G, by analyzing the DOS of the spin-polarized electrons, this circumstance can be explained as the Fermi level could be manipulated by moderate carrier doping by varying the amount of unpaired spin-up states, which consequently affects the magnetic moment[153]. In addition, when an external magnetic field is applied vertically and parallel to the plane, the corresponding magnetoresistance effect on $Cr_2Ge_2Te_6$ changes from positive to negative, which exhibits an exchange interaction from carriers and local moments[167].

Figure 9H and I show that for ferromagnetism in the $Cr_2Ge_2Te_6$ family, the spin moments on the Cr sitesmainly interact through the indirect 90° super-exchange coupling of the Cr dz^2-Te p-Cr dz^2 path[168]. The ligand p spin-orbit coupling contributes to weak FM coupling. Based on DFT calculations and the Hamiltonian and tight-binding models, the total Hamiltonian of the 2D $Cr_2Ge_2Te_6$ system contains two main factors, namely, the exchange interaction and single-ion anisotropy, with the former being regarded as a combination of the isotropy change and Kitaev interaction. Among them, it was found that the single-ion anisotropy and the Kitaev interaction could be attributed to the heavy ligand of Te that leads to SOC in $Cr_2Ge_2Te_6$[161]. This may be the reason why the critical transition temperature in 2D $Cr_2Ge_2Te_6$ can be consciously tuned by an external magnetic field and thickness. Using DFT, the competitive relationship of MAE and dipolar anisotropy energy can explain the lack of spontaneous magnetization in monolayer $Cr_2Ge_2Te_6$[169]. With a slight change in the Cr-Te bonding, a small out-of-plane anisotropy could be introduced in this 2D Heisenberg ferromagnet[95]. Despite the existence of vdW spacing along the c-axis, its interlayer magnetic coupling cannot be ignored in view of the strong dimensional-dependent T_c of $Cr_2Ge_2Te_6$ for different thicknesses. Like $Cr_2Ge_2Te_6$, studies have shown that $Cr_2Si_2Te_6$[57] and $Cr_2Sn_2Te_6$[54] have similar performance in terms of magnetic anisotropy and phase transition temperature. Furthermore, topologically nontrivial magnetic spin states known as skyrmion bubbles with homochirality in layered $Cr_2Ge_2Te_6$ contribute to the dipolar interaction and uniaxial magnetic anisotropy[170]. There are two kinds of spins

isolated in each Bloch domain with a topological charge of ±1.

Manipulating and utilizing ferromagnetic performance has been of great importance for many model systems. For example, the driving of an external electric field enabled the tunable bipolar magnetism by rebalancing the spin-polarized band structure by shifting the Fermi level[153]. A strain-induced structural distortion by detecting the change in spin-phonon coupling showed the modulation of spin-lattice coupling and magnetostrictions for $Cr_2Si_2Te_6$[57], $Cr_2Ge_2Te_6$[171], and Fe_3GeTe_2[172]. Another approach is the employment of the magnetic proximity effect by constructing vdW moiré superlattices that tune the spin-dependent interlayer orbital coupling. This heteroatomic distribution by moiré periodicity via twisting or strain between the adjacent layers brings about a lateral modulation of a magnetic proximity field and develops a miniband splitting of spin[173]. Furthermore, a theoretical investigation of the magneto-optical effect in layered $Cr_2Ge_2Te_6$ also described the calculations of optical conductivity and the magneto-optical Kerr and Faraday effects[169]. Furthermore, according to the magnetic Cr dopant into Bi_2Se_3, a gap opening in the 2D Dirac surface states in a 3D topological insulator may give rise to quantum anomalous Hall states on 1D edges by TRS breaking[174]. Moreover, endeavors have been attempted via growing topological insulators onto $Cr_2Ge_2Te_6$ by MBE growth[175]. These fundamental behaviors suggest that 2D $Cr_2Ge_2Te_6$ presents multiple intriguing physical properties that can be widely used in various scientific fields.

Ternary iron germanium telluride Fe_3GeTe_2

Fe_3GeTe_2 is an itinerant ferromagnet that can reach a monolayer with strong c-axis out-of-plane anisotropy and has a T_c of ~220 K in the bulk form[176]. There are two inequivalent Fe ions with different degrees of localization that contribute to different magnetic moments[177]. Figure 10A and B show the hexagonal structure with three-atom-thick Fe_3Ge with Fe (I)-Fe (II) and Fe (I)-Ge bonding sandwiched by two weak vdW interaction layers of Te anions. In particular, the monolayer thick Fe_3GeTe_2 exhibits significant uniaxial magnetocrystalline anisotropy energy, with Fe atoms in each layer of 920 meV[172]. With the existence of Fe vacancies, the T_c and magnetic anisotropy of the produced Fe_3GeTe_2 decrease[178].

Magnetic analysis showed that the strong SOC counts for the c-axis magnetic anisotropy with ferromagnetic spin aligned in each layer[44]. The anomalous Hall effect (AHE) test in Figure 10C-E shows an almost perfect square hysteresis loop under the application of an external field along the c-axis, particularly for thickness less than 200 nm, and its coercive field reduces with increasing temperature until totally disappearing over T_C, which suggests a hard magnetic behavior for bulk Fe_3GeTe_2[37]. Furthermore, the ferromagnetic analysis showed a strong dependence on the thickness of Fe_3GeTe_2 and an indication of an effective interlayer coupling length that is less than five layers. The detection of a decreased T_c for monolayer Fe_3GeTe_2 by magnetic circular dichroism[179] and AHE[44] results [Figure 10C-F] revealed the survival of the magnetic order and may have been influenced by the difference in the electron density[180]. As reported, Fe_3GeTe_2 is a metal with a carrier concentration of 1.2×10^{19} cm^{-3} in MBE grown samples (with carrier mobility of ~50 $cm^2 \cdot V^{-1} \cdot s^{-1}$) and ~$10^{21}$ cm^{-3} (~8×10^{13} cm^{-2} per layer) in the chemical vapor transport grown samples[91]. An experiment evidenced a carrier doping method into trilayer $Fe_{3-x}GeTe_2$ via ionic gating contributed to a dramatic increase of T_c over ambient temperature[179]. These recent advances accelerate the realization of ambient stable 2D magnets down to the monolayer limit.

The strong dimensionality dependence on the itinerant ferromagnetism in Fe_3GeTe_2 revealed a transition from the 3D to 2D Ising model when the thickness was less than five layers, accompanied by a rapid drop of T_c. The magnetic ground state of monolayer FGT is determined by direct exchange and super-exchange competition[181]. On the one hand, the *d* orbitals on the nearest-neighbored Fe atoms overlap directly, making up the direct exchange interaction of AFM Fe-Fe coupling in FGT. On the other hand, the *d* orbitals

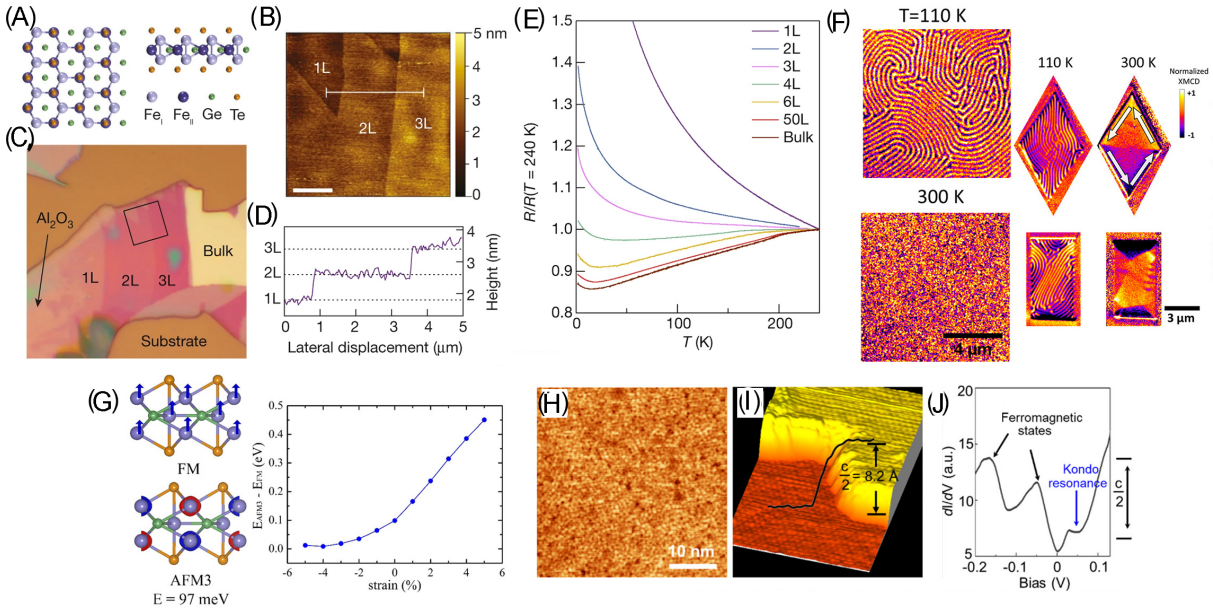

Figure 10. (A) Schematic of atomic structure of monolayer Fe_3GeTe_2. (B) AFM image, (C) optical image and (D) cross-sectional profile of the selected area in few-layer flakes of Fe_3GeTe_2. (E) Temperature-dependent sample resistance of Fe_3GeTe_2 [44]. (F) Photoemission electron microscopy topography image of magnetic-stripe domains of Fe_3GeTe_2 at different temperatures, sizes and shapes[180]. (G) FM and AFM configurations and spin-density distribution in Fe_3GeTe_2 monolayer and their energy difference between the two couplings[181]. (H) Large-scale and (I) atom resolved STM images and the (J) dI/dV curve of the surface of Fe_3GeTe_2 [182].

of the nearest-neighbored Fe atoms overlap indirectly via the p orbitals of Ge or Te atoms, making up a super-exchange interaction of FM Fe-Ge/Te coupling. The Fe-Ge and Fe-Te bonds are stronger than that of Fe-Fe, and as a consequence, the FM super-exchange interaction prevails over the direct AFM exchange interaction, as shown in Figure 10G[181].

Typically, the interlayer exchange coupling in Fe_3GeTe_2 is much weaker but may have a contribution to a 3D critical behavior in sufficient multiple layers. Considering the existence of intrinsic anisotropy, the long-range magnetic order in the monolayer limit is supposed to be maintained, leading to the diversity of Tc with dimension crossover from 3D to 2D. For example, the magnetic anisotropy originates from a strong SOC and magnetostatic dipole-dipole interaction that is strong enough to stabilize the 2D ferromagnetism. It is noteworthy that a heavy-fermion behavior from exchange splitting is confirmed by a massive spectral weight transfer in the 3*d* electrons of Fe_3GeTe_2, as shown in Figure 10H-J[182], as well as a Kondo lattice behavior proved by the character of Fano resonance[183]. These phenomena not only describe the relationship between the Kondo screening effect and Ising ferromagnetism but also reveal the origin of the heavy-fermion behavior in the 3*d*-electron vdW Fe_3GeTe_2 [183]. This coexistence of itinerant electrons and local magnetic moments possibly contributes to extensive research on strong correlation phases in 3*d*-electron systems[95].

Owing to the unique properties of vdW Fe_3GeTe_2, it exhibits exceptional behavior that permits the development of many magnetism-related studies. For hole doping, the occupation degree and splitting of ferromagnetic Fe-Te bonding significantly influence the magnetic anisotropy in FGT[184]. Furthermore, the strong magnetoelastic coupling in the magnetostrictive Fe_3GeTe_2 monolayer suggests an improvement of magnetic anisotropy energy via utilizing a 2% structural tensile strain[172]. For example, a pulse-current induced magnetization reversal was recently found in a Fe_3GeTe_2 homojunction with reduced coercivity by spin-orbit torque and Joule heat[185]. Moreover, when considering the magnetic proximity, the contact

strength, and electric and magnetic behaviors, electronic and spin injection are determined by the bond and match type of their introduced substrates[186]. Another interesting phenomenon in vdW Fe_3GeTe_2 lies in its shape of magnetic domain with different hysteresis loops. The thickness-dependent stripe domain phase in Figure 10F suggests the quasi-2D magnetic behaviors in Fe_3GeTe_2, as well as an indication of long-range dipolar interaction over the exchange interaction and magnetic anisotropy[180,187]. In addition, at a certain thickness and temperature, a labyrinthine domain structure emerges[188]. Interestingly, a topological spin texture of magnetic skyrmions was observed in Fe_3GeTe_2 vdW flakes and further revealed finite interfacial Dzvaloshinskii-Moriya interactions that confirm the spin chirality. Furthermore, a large anomalous Nernst effect, an evident spin-phonon coupling effect, and enhanced electronic specific heat enrich the complex phase diagram, enabling fertile grounds for massive emergent phenomena and applications of Fe_3GeTe_2.

The genuine magnetic origin of vdW Fe_3GeTe_2 is still debated. First, there is no consensus regarding long-range order over ferromagnetic or antiferromagnetic[83]. Second, when describing the magnetic behavior in various conditions, the consistency among calculation and measurement results is not satisfactory. Finally, there is still a lack of clear evidence of describing the magnetic behavior after completely removing the unexpected ferromagnetic impurities.

Ternary manganese bismuth telluride ($MnBi_{2n}Te_{3n+1}$, n = 1, 2 or 3)

The layered manganese bismuth telluride ($MnBi_{2n}Te_{3n+1}$) family possesses combinations of intrinsic magnetism and nontrivial topological insulator (TI), hosting interesting physical effects, such as A-type antiferromagnetism [Figure 11A], intrinsic axion insulator states, a quantum anomalous Hall state and a quantized topological magnetoelectric effect[189]. The magnetism coupling with topology accommodates a vast space to explore exotic topics related to quantum effects in condensed matter physics[7].

Atomically thin $MnBi_2Te_4$ has a heptalayer structure, forming a Te-Bi-Te-Mn-Te-Bi-Te stacking along the out-of-plane axis. Similar to the architecture of 1T-ASe_2, the magnetic Mn cations and the nearest layered Te atoms form a triangular lattice at the center of the heptalayer. Similar materials, like $MnBi_{2n}Te_{3n+1}$, can be briefly considered as charge-balanced alternating stacking of monolayer $MnBi_2Te_4$ and few-layer Bi_2Te_3. Layered $MnBi_2Te_4$ presents intralayer FM and A-type interlayer AFM of Mn coupling along the c-axis below 25 K[80]; for the $MnBi_4Te_7$ and $MnBi_6Te_{10}$, the Néel temperature T_N can be lowered down to 13 and 11 K, respectively. Viewing the opposite parities of studies shows that the multiple states of magnetism in $MnBi_{2n}Te_{3n+1}$ can be realized by applying different external fields and temperatures. When the outer magnetic field increases over 3.5 T at 2 K, the $MnBi_2Te_4$ experience a spin-flip transition from the layered AFM ground state to a canted AFM, with spin oriented out-of-plane and in-plane components aligning oppositely between the neighboring slabs. The same spin-flip can be seen at ~0.15 and 0.01 T for $MnBi_4Te_7$ and $MnBi_6Te_{10}$, respectively[190], demonstrating a declined AFM interlayer exchange interaction as the interlayer distance increases. This further proves the favor of manipulating the FM coupling via changing the short-range adjacent layer AFM coupling and the strength of magnetic anisotropy.

In the bulk form of AFM $MnBi_2Te_4$, shown in Figure 11B and C, a band inversion of first close and then reopen behavior can be inferred in view of the opposite parities of valence band maximum and conduction band minimum at Γ point and the reversed signs with the strength changes in SOC[189]. With the presence of spontaneous magnetic moments integrated by SOC that no requirement of the external magnetic field in Figure 11D and E, a topologically nontribal band structure could exhibit an exotic transport phenomenon of the quantum anomalous Hall effect. Together with the magnetic performance, the topological phases evolve with varying thickness of the stacking layer. DFT calculations indicated a quantum anomalous Hall (QAH) insulator behavior in odd-layered $MnBi_2Te_4$ and an axion insulator behavior in an even-layered sample[12].

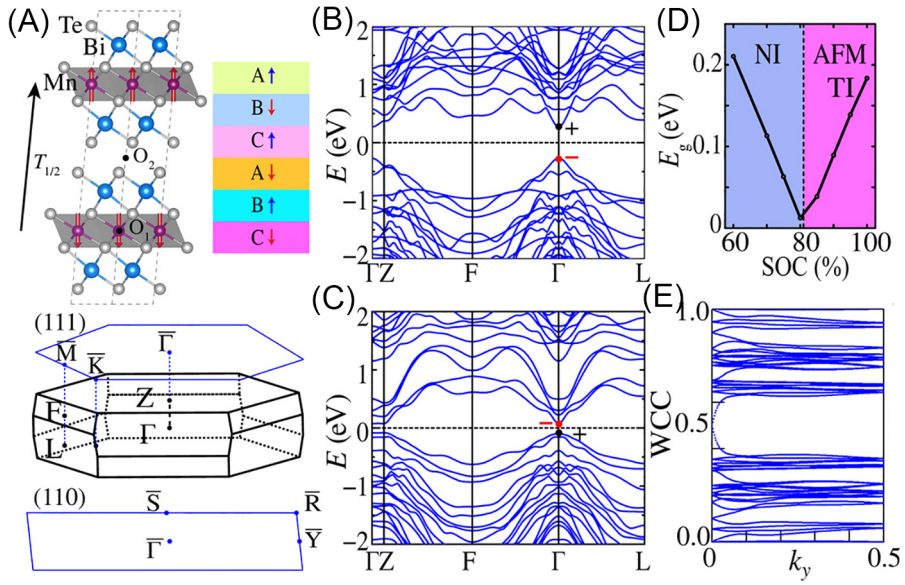

Figure 11. (A) Crystal structure of bulk AFM $MnBi_2Te_4$ with high symmetry points in reciprocal space. Band structures profiles (B) without SOC and (c) with SOC. (D) SOC-dependent band gap energy at Γ, showing an evolution from a trivial insulator to a topological insulator by changing the SOC. (E) Wannier charge center evolving with k_y, referring to a nonzero topological invariant[189].

Furthermore, a QAH experiment on a hexalayered $MnBi_2Te_4$ sample had seen the axion insulator state with Hall resistivity was offset by the pair of top and bottom surfaces that cancel each other. Simultaneously, a nine-layer $MnBi_2Te_4$ device was also found to exhibit a Chern insulator phase[73], i.e., the members of $MnBi_{2n}Te_{3n+1}$ reveal various topological states that can be complementarily and synthetically. In short, the magnetism coupling with topology would accommodate vast space to explore exotic topics related to quantum effects in condensed matter physics[7].

Advances in heterostructure applications

With the advantages of easy access, good flexibility, controllable interlayer twisting and stacking, and few lattice mismatch, 2D vdW magnets provide a convenient platform for condensed matter physics and potential applications by interfacial engineering. In turn, to manipulate the magnetic properties, constructing heterostructures can effectively adjust the electronic structure in atomically thin films. Such artificial materials provide tremendous freedom to design, construct, manipulate and apply novel physical properties and devices[191]. As shown in Figure 12, the elementary functions of 2D materials enable some advanced development of spintronics, including generating and detecting spin-charge conversion, spin transport, and manipulation, which requires a material itself to possess good nature with high carrier mobility, long spin lifetime, and long diffusion distances[192].

For interfacial engineering, exchange proximity represents one of the main effects in many vdW heterostructures devices, such as switching the Schottky barrier height in In_2Se_3/Fe_3GeTe_2[193], giant tunneling magnetoresistance that accommodates spin-filter tunnel barriers[33], adjusting the tunneling electroresistance in the 2D FM Schottky heterojunction[194,195], generating exchange bias effect in $CrCl_3/Fe_3GeTe_2$[196] and valley manipulation by CrI_3/WSe_2 heterostructures[118]. In addition, combining ferromagnetic insulators and superconductors have opportunities to produce triplet and even topological superconductivity[197], as well as the Andreev reflection at the interface of FM vdW/superconductor[198,199]. Another consideration is to generate QAHE; due to the atomic flat and regardless of the electronic

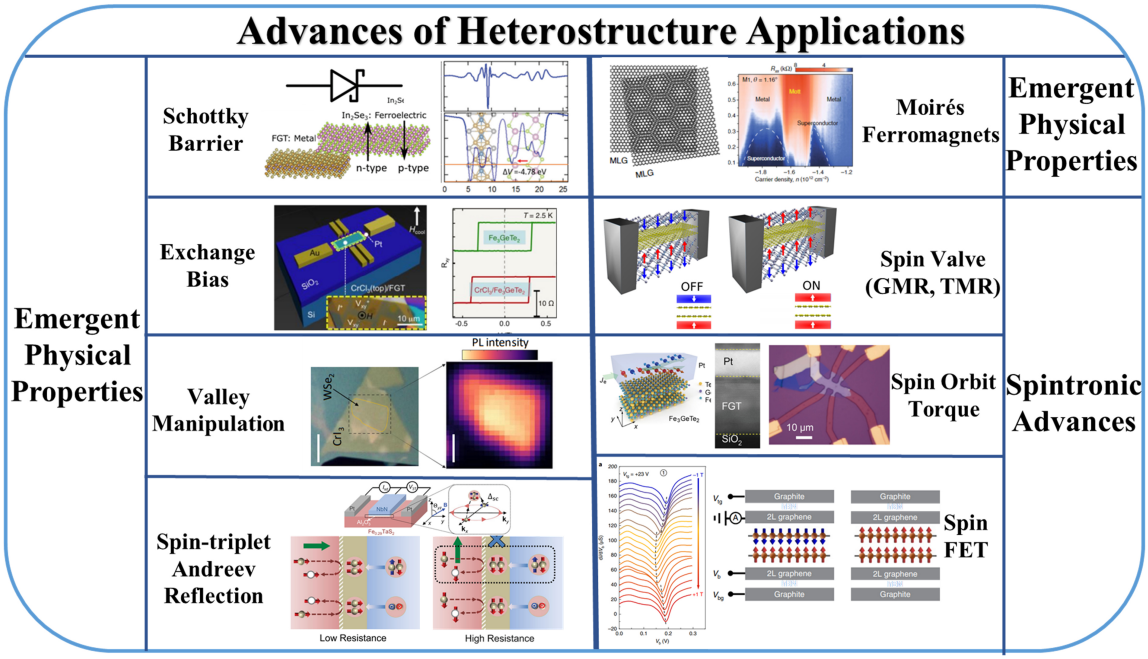

Figure 12. Applications of 2D ferromagnets in vdW heterostructures and twisted lattices, including emergent physical properties of tuning the Schottky barrier height[193], exchange bias[196], valley manipulation[118], anisotropic spin-triplet Andreev reflection[198] and anisotropic strong correlation moiré flat bands[202], as well as spintronic devices, such as spin valves[204], spin-orbit torque[209] and spin field-effect transistors[36].

scattering, the vdW ferromagnet is ideal for introducing magnetism into quantum spin Hall effect topological insulator. Such efforts have been attempted by chemical vapor depositing Bi_2Te_3 on $Cr_2Ge_2Te_6$[200] and epitaxy growth of $Cr_2Ge_2Te_6$ on $(Bi,Sb)_2Te_3$[175]. Moreover, magnetic multilayers, moiré[201,202] and twisted 2D magnet[203] engineering can produce an additional degree of freedom in epitaxially growing metallic heterostructures and have an enormous potential for new physical phenomena.

Constructing magnetically coupled structures provides a promising platform for spintronics regardless of crystal mismatch. For instance, first, when a nonmagnetic layer has parallel/antiparallel spin polarization at its two sandwiching interfaces with a ferromagnet, it makes up a spin valve setup that corresponds to two switching configurations, such as variation of magnetoresistance and spin filtering effect[204]. Currently, these spin filtering effect magnetic tunnel junction (MTJ) exhibit tunneling magnetoresistance in dual-gated quadra-layer CrI_3 spin-filter MTJ[205] and tunneling spin-valve Fe_3GeTe_2/h-BN/Fe_3GeTe_2 heterostructure[6], as well as a giant magnetoresistance effect in Fe_3GeTe_2/MoS_2/Fe_3GeTe_2 heterostructures[206]. Interestingly, a prediction also claimed a similar FM insulator/superconductor/ FM insulator that can give insight into relations between superconductivity and ferromagnetism, which is waiting to be realized[207]. Second, at the heavy-metal/ferromagnet interface, a spin-orbit torque can be produced by a spin Hall or Rashba effect that could generate an in-plane spin current and switch the magnetization direction[208]. For example, the vertical magnetization of Fe_3GeTe_2 in Fe_3GeTe_2/Pt can be tuned by alternating the current direction in the Pt layer[209]; a similar conclusion was drawn by Johansen's theoretical discussion and proposed a qualitative relationship between current and the critical temperature that has the possibility to realize the BKT phase transition[210]. Another heterostructure application of 2D ferromagnet potential is to attribute the spin nature to the spin logic gate devices, one of which solution is to form a spin field-effect transistor (s-FET). With ferromagnetic drain and source electrodes, the spin polarization of the current in the 2D electron gas

channel can be modulated by the selected electrical gate voltage in a dual-gated graphene/CrI_3/graphene s-FET[36]. Finally, in view of alternating the spin through the device requires only low energy dissipation within a very fast time, s-FET is considered a promising 2D spintronic candidate with low power consumption and high computing output.

CONCLUSIONS

2D ferromagnets have become a research hotspot and triggered the exploration of peculiar quantum phenomena in more and more fields, leading to numerous frontier disciplines being integrated and improved. This review first considered 2D magnetic materials and 2D ferromagnetism by discussing their emerging and interaction mechanisms, physical property features, and corresponding manipulations. Then, from this standpoint, we examined the interplay in several synthesized ferromagnetic vdW families in detail. This will not only bring novel basic physics, contributing to developing more research and technology in magnetism but also greatly expands the practice of 2D materials.

Here, we need to determine the key issues so far that require solutions in priority. First, to further expand the atomically thin magnet families, there is still a lack of sufficient experimental evidence for validating the long-standing theoretical forecasts in real 2D systems. This includes understanding the exchange mechanism of 2D ferromagnets, manipulating complex magnetic sequences, designing and predicting new 2D ferromagnets, and understanding interface and proximity effects. Furthermore, rigorously predicting the thermodynamic stability of the crystallographic and magnetic subsystems in 2D magnets is still a lofty goal, and theoretical advances in computing-driven material design are needed and further improved. Second, broadening the spectrum of compounds is still in need of adequate experimental investigations, including the synthesizing and exfoliating of novel van der Waals magnets. Additionally, controllable achieving large-size, high quality and productivity, and uniformly distributed crystal growth have remained a huge challenge. Third, for the practical application of heterostructure devices, the realization of the robust ambient magnetic order adjustment in atmospheric conditions, thoroughly understanding the interplay of 2D ferromagnetism, introducing quantum band topology, and modifying the electric field manipulating of charge carriers and spins is meant to be overcome, especially when determining the key factors for the many-body issues. In the long term, the integration and association of this 2D magnet with other functional materials are essential for expanding applications.

The current work on 2D magnetic materials mainly contains four aspects: the synthesis and characterization of novel magnetic 2D materials; the origin and mechanism of magnetism; the adjustment of basic characteristics; applications. Similarly, the fields of 2D ferromagnetism of non-van der Waals and thin-film materials, multiferroic materials, quantum spin liquids, topological insulators, and Chen insulators, the frustrating material, the interaction between magnetism and topology under twisted proximity effect are also worthy of paying attention and importance. Future research still demands multiple technological developments and new ideas to realize the formation, detection, and application of magnetism under extreme conditions.

In summary, the exploration of 2D magnetic materials and 2D ferromagnetism represents a marvelously versatile and fertile field that can be used to pursue many fascinating physical phenomena and the realization of multiple device concepts. The influence of this technique will be far-reaching, with numerous challenges and opportunities coexisting.

DECLARATIONS

Acknowledgments

The authors acknowledge the support from the BUAA-UOW Joint Research Centre. This work was supported by National Natural Science Foundation of China (Nos. 11874003, 12074021, 11974036, 11834014, 11904015, and 51672018), Beijing Natural Science Foundation (Z180007), National Key R&D Program of China (2018YFE0202700), and the Australian Research Council (LP180100722).

Authors' contributions

Made substantial contributions to conception and design of the study: Du Y, Hao W, Zhuang J, Xu X
Performed data acquisition and writing: Xu H, Xu S, Du Y, Hao W, Zhuang J

Availability of data and materials

Not applicable.

Financial support and sponsorship

National Natural Science Foundation of China (Nos. 11874003, 12074021, 11974036, 11834014, 11904015, and 51672018), Beijing Natural Science Foundation (Z180007), National Key R&D Program of China (2018YFE0202700), and the Australian Research Council (LP180100722).

Conflicts of interest

All authors declared that there are no conflicts of interest.

Ethical approval and consent to participate

Not applicable.

Consent for publication

Not applicable.

REFERENCES

1. Novoselov KS, Geim AK, Morozov SV, et al. Electric field effect in atomically thin carbon films. *Science* 2004;306:666-9. DOI PubMed
2. Novoselov KS, Mishchenko A, Carvalho A, Castro Neto AH. 2D materials and van der Waals heterostructures. *Science* 2016;353:aac9439. DOI PubMed
3. Nikonov KS, Brekhovskikh MN, Egorysheva AV, Menshchikova TK, Fedorov VA. Chemical vapor transport growth of vanadium(IV) selenide and vanadium(IV) telluride single crystals. *Inorg Mater* 2017;53:1126-30. DOI
4. Chen B, Yang J, Wang H, et al. Magnetic properties of layered itinerant electron ferromagnet Fe_3 $GeTe_2$. *J Phys Soc Jpn* 2013;82:124711. DOI
5. Zhang X, Zhao Y, Song Q, Jia S, Shi J, Han W. Magnetic anisotropy of the single-crystalline ferromagnetic insulator Cr_2 Ge_2 Te_6. *Jpn J Appl Phys* 2016;55:033001. DOI
6. Wang Z, Sapkota D, Taniguchi T, Watanabe K, Mandrus D, Morpurgo AF. Tunneling spin valves based on Fe_3GeTe_2/hBN/Fe_3GeTe_2 van der Waals heterostructures. *Nano Lett* 2018;18:4303-8. DOI PubMed
7. Liu C, Wang Y, Li H, et al. Robust axion insulator and Chern insulator phases in a two-dimensional antiferromagnetic topological insulator. *Nat Mater* 2020;19:522-7. DOI PubMed
8. Kong T, Stolze K, Timmons EI, et al. VI_3-a new layered ferromagnetic semiconductor. *Adv Mater* 2019;31:e1808074. DOI PubMed
9. Huang C, Feng J, Wu F, et al. Toward intrinsic room-temperature ferromagnetism in two-dimensional semiconductors. *J Am Chem Soc* 2018;140:11519-25. DOI PubMed
10. Gong C, Li L, Li Z, et al. Discovery of intrinsic ferromagnetism in two-dimensional van der Waals crystals. *Nature* 2017;546:265-9. DOI PubMed
11. Otrokov MM, Klimovskikh II, Bentmann H, et al. Prediction and observation of an antiferromagnetic topological insulator. *Nature*

2019;576:416-22. DOI PubMed
12. Otrokov MM, Rusinov IP, Blanco-Rey M, et al. Unique thickness-dependent properties of the van der Waals interlayer antiferromagnet $MnBi_2Te_4$ films. *Phys Rev Lett* 2019;122:107202. DOI PubMed
13. Tsen AW, Hunt B, Kim YD, et al. Nature of the quantum metal in a two-dimensional crystalline superconductor. *Nature Phys* 2016;12:208-12. DOI
14. Song Q, Occhialini CA, Ergeçen E, et al. Evidence for a single-layer van der Waals multiferroic. *Nature* 2022;602:601-5. DOI PubMed
15. Fumega AO, Gobbi M, Dreher P, et al. Absence of ferromagnetism in VSe_2 caused by its charge density wave phase. *J Phys Chem C* 2019;123:27802-10. DOI
16. Xi X, Zhao L, Wang Z, et al. Strongly enhanced charge-density-wave order in monolayer $NbSe_2$. *Nat Nanotechnol* 2015;10:765-9. DOI PubMed
17. Chen L, Chung J, Gao B, et al. Topological spin excitations in honeycomb ferromagnet CrI_3. *Phys Rev X* 2018:8. DOI
18. Cao Q, Yun FF, Sang L, Xiang F, Liu G, Wang X. Defect introduced paramagnetism and weak localization in two-dimensional metal VSe_2. *Nanotechnology* 2017;28:475703. DOI PubMed
19. Liu H, Bao L, Zhou Z, et al. Quasi-2D transport and weak antilocalization effect in few-layered VSe_2. *Nano Lett* 2019;19:4551-9. DOI PubMed
20. Wu Y, Zhang S, Zhang J, et al. Néel-type skyrmion in WTe_2/Fe_3GeTe_2 van der Waals heterostructure. *Nat Commun* 2020;11:3860. DOI PubMed PMC
21. Liu Y, Weiss NO, Duan X, et al. Van der Waals heterostructures and devices. *Nat Rev Mater* 2016;1:1-17. DOI
22. Thiel L, Wang Z, Tschudin MA, et al. Probing magnetism in 2D materials at the nanoscale with single-spin microscopy. *Science* 2019;364:973-6. DOI PubMed
23. Avsar A, Ochoa H, Guinea F, Özyilmaz B, van Wees B, Vera-marun I. Colloquium: Spintronics in graphene and other two-dimensional materials. *Rev Mod Phys* 2020;92:021003. DOI
24. Tokura Y, Yasuda K, Tsukazaki A. Magnetic topological insulators. *Nat Rev Phys* 2019;1:126-43. DOI
25. Tannous C, Comstock RL. Magnetic information-storage materials. In: Kasap S, Capper P, editors. Springer Handbook of Electronic and Photonic Materials. Cham: Springer International Publishing; 2017. p. 1. DOI
26. Mcguire MA, Dixit H, Cooper VR, Sales BC. Coupling of crystal structure and magnetism in the layered, ferromagnetic insulator CrI_3. *Chem Mater* 2015;27:612-20. DOI
27. Banerjee A, Bridges CA, Yan JQ, et al. Proximate Kitaev quantum spin liquid behaviour in a honeycomb magnet. *Nat Mater* 2016;15:733-40. DOI PubMed
28. Zhou P, Sun CQ, Sun LZ. Two dimensional antiferromagnetic Chern insulator: $NiRuCl_6$. *Nano Lett* 2016;16:6325-30. DOI PubMed
29. Zhang X, Zhao X, Wu D, Jing Y, Zhou Z. $MnPSe_3$ monolayer: a promising 2D visible-light photohydrolytic catalyst with high carrier mobility. *Adv Sci (Weinh)* 2016;3:1600062. DOI PubMed PMC
30. Desai SB, Madhvapathy SR, Amani M, et al. Gold-mediated exfoliation of ultralarge optoelectronically-perfect monolayers. *Adv Mater* 2016;28:4053-8. DOI PubMed
31. Yang K, Hu W, Wu H, Whangbo M, Radaelli PG, Stroppa A. Magneto-optical kerr switching properties of $(CrI_3)_2$ and $(CrBr_3/CrI_3)$ bilayers. *ACS Appl Electron Mater* 2020;2:1373-80. DOI
32. Zhong D, Seyler KL, Linpeng X, et al. Layer-resolved magnetic proximity effect in van der Waals heterostructures. *Nat Nanotechnol* 2020;15:187-91. DOI PubMed
33. Song T, Cai X, Tu MW, et al. Giant tunneling magnetoresistance in spin-filter van der Waals heterostructures. *Science* 2018;360:1214-8. DOI PubMed
34. Gong Y, Liu Z. Preface to the special issue on tungsten-and molybdenum-based two-dimensional materials for energy storage and conversion. *Tungsten* 2020;2:107-8. DOI
35. Luo G, Lu G, Liu X. Preface to the special issue on plasma facing materials for fusion energy. *Tungsten* 2019;1:121-121. DOI
36. Jiang S, Li L, Wang Z, Shan J, Mak KF. Spin tunnel field-effect transistors based on two-dimensional van der Waals heterostructures. *Nat Electron* 2019;2:159-63. DOI
37. Tombros N, Jozsa C, Popinciuc M, Jonkman HT, van Wees BJ. Electronic spin transport and spin precession in single graphene layers at room temperature. *Nature* 2007;448:571-4. DOI PubMed
38. Sun Y, Zhuo Z, Wu X, Yang J. Room-temperature ferromagnetism in two-dimensional Fe_2Si nanosheet with enhanced spin-polarization ratio. *Nano Lett* 2017;17:2771-7. DOI PubMed
39. Escolar J, Peimyoo N, Craciun MF, et al. Anisotropic magnetoconductance and coulomb blockade in defect engineered $Cr_2Ge_2Te_6$ van der Waals heterostructures. *Phys Rev B* 2019:100. DOI
40. Miao GX, Müller M, Moodera JS. Magnetoresistance in double spin filter tunnel junctions with nonmagnetic electrodes and its unconventional bias dependence. *Phys Rev Lett* 2009;102:076601. DOI PubMed
41. Alghamdi M, Lohmann M, Li J, et al. Highly efficient spin-orbit torque and switching of layered ferromagnet Fe_3GeTe_2. *Nano Lett* 2019;19:4400-5. DOI PubMed
42. Li LJ, O'Farrell EC, Loh KP, Eda G, Özyilmaz B, Castro Neto AH. Controlling many-body states by the electric-field effect in a two-dimensional material. *Nature* 2016;529:185-9. DOI PubMed
43. Hu W, Yang K, Stroppa A, Continenza A, Wu H. 2D hybrid $CrCl_2(N_2C_4H_4)_2$ with tunable ferromagnetic half-metallicity. *J Mater*

Chem C 2021;9:5985-91. DOI

44. Deng Y, Yu Y, Song Y, et al. Gate-tunable room-temperature ferromagnetism in two-dimensional Fe_3GeTe_2. *Nature* 2018;563:94-9. DOI PubMed
45. Zhang C, Nie Y, Sanvito S, Du A. First-principles prediction of a room-temperature ferromagnetic janus VSSe monolayer with piezoelectricity, ferroelasticity, and large valley polarization. *Nano Lett* 2019;19:1366-70. DOI PubMed
46. Hohenberg PC. Existence of long-range order in one and two dimensions. *Phys Rev* 1967;158:383-6. DOI
47. Mermin ND, Wagner H. Absence of ferromagnetism or antiferromagnetism in one- or two-dimensional isotropic heisenberg models. *Phys Rev Lett* 1966;17:1133-6. DOI
48. Lines ME. Magnetism in two dimensions. *Journal of Applied Physics* 1969;40:1352-8. DOI
49. Kohlhepp J, Elmers HJ, Cordes S, Gradmann U. Power laws of magnetization in ferromagnetic monolayers and the two-dimensional Ising model. *Phys Rev B Condens Matter* 1992;45:12287-91. DOI PubMed
50. Pacilé D, Meyer JC, Girit ÇÖ, Zettl A. The two-dimensional phase of boron nitride: Few-atomic-layer sheets and suspended membranes. *Appl Phys Lett* 2008;92:133107. DOI
51. Li L, Yu Y, Ye GJ, et al. Black phosphorus field-effect transistors. *Nat Nanotechnol* 2014;9:372-7. DOI PubMed
52. Naguib M, Kurtoglu M, Presser V, et al. Two-dimensional nanocrystals produced by exfoliation of Ti_3AlC_2. *Adv Mater* 2011;23:4248-53. DOI
53. Manzeli S, Ovchinnikov D, Pasquier D, Yazyev OV, Kis A. 2D transition metal dichalcogenides. *Nat Rev Mater* 2017;2:17033. DOI
54. Zhuang HL, Xie Y, Kent PRC, Ganesh P. Computational discovery of ferromagnetic semiconducting single-layer $CrSnTe_3$. *Phys Rev B* 2015:92. DOI
55. Ge Y, Zhu Z, Xu Y, et al. Broadband nonlinear photoresponse of 2D TiS_2 for ultrashort pulse generation and all-optical thresholding devices. *Advanced Optical Materials* 2018;6:1701166. DOI
56. Joy PA, Vasudevan S. Magnetism in the layered transition-metal thiophosphates MPS_3 (M = Mn, Fe, and Ni). *Phys Rev B Condens Matter* 1992;46:5425-33. DOI PubMed
57. Casto LD, Clune AJ, Yokosuk MO, et al. Strong spin-lattice coupling in $CrSiTe_3$. *APL Materials* 2015;3:041515. DOI
58. Lado JL, Fernández-rossier J. On the origin of magnetic anisotropy in two dimensional CrI_3. *2D Mater* 2017;4:035002. DOI
59. Grönke M, Buschbeck B, Schmidt P, et al. Chromium trihalides Cr. *X* ;6:1901410. DOI
60. Cai X, Song T, Wilson NP, et al. Atomically thin $CrCl_3$: an in-plane layered antiferromagnetic insulator. *Nano Lett* 2019;19:3993-8. DOI PubMed
61. Huang B, Clark G, Navarro-Moratalla E, et al. Layer-dependent ferromagnetism in a van der Waals crystal down to the monolayer limit. *Nature* 2017;546:270-3. DOI PubMed
62. Zhou Y, Wang Z, Yang P, et al. Tensile strain switched ferromagnetism in layered NbS_2 and $NbSe_2$. *ACS Nano* 2012;6:9727-36. DOI PubMed
63. Chua R, Yang J, He X, et al. Can reconstructed se-deficient line defects in monolayer VSe_2 induce magnetism? *Adv Mater* 2020;32:e2000693. DOI PubMed
64. Bonilla M, Kolekar S, Ma Y, et al. Strong room-temperature ferromagnetism in VSe_2 monolayers on van der Waals substrates. *Nat Nanotechnol* 2018;13:289-93. DOI PubMed
65. Meng L, Ma Y, Si K, Xu S, Wang J, Gong Y. Recent advances of phase engineering in group VI transition metal dichalcogenides. *Tungsten* 2019;1:46-58. DOI
66. Ding X, Liu T, Ahmed S, Bao N, Ding J, Yi J. Enhanced ferromagnetism in WS_2 via defect engineering. *Journal of Alloys and Compounds* 2019;772:740-4. DOI
67. Yun SJ, Duong DL, Ha DM, et al. Ferromagnetic order at room temperature in monolayer WSe_2 semiconductor via vanadium dopant. *Adv Sci (Weinh)* 2020;7:1903076. DOI PubMed PMC
68. Tongay S, Varnoosfaderani SS, Appleton BR, Wu J, Hebard AF. Magnetic properties of MoS_2: existence of ferromagnetism. *Appl Phys Lett* 2012;101:123105. DOI
69. Xia B, Gao D, Liu P, Liu Y, Shi S, Tao K. Zigzag-edge related ferromagnetism in $MoSe_2$ nanoflakes. *Phys Chem Chem Phys* 2015;17:32505-10. DOI PubMed
70. Liu W, Dai Y, Yang Y, et al. Critical behavior of the single-crystalline van der Waals bonded ferromagnet $Cr_2Ge_2Te_6$. *Phys Rev B* 2018:98. DOI
71. Blei M, Lado JL, Song Q, et al. Synthesis, engineering, and theory of 2D van der Waals magnets. *Applied Physics Reviews* 2021;8:021301. DOI
72. Park SY, Kim DS, Liu Y, et al. Controlling the magnetic anisotropy of the van der Waals ferromagnet Fe_3GeTe_2 through hole doping. *Nano Lett* 2020;20:95-100. DOI PubMed
73. Zhang RX, Wu F, Das Sarma S. Möbius insulator and higher-order topology in MnBi2nTe3n+1. *Phys Rev Lett* 2020;124:136407. DOI PubMed
74. Mak KF, Shan J, Ralph DC. Probing and controlling magnetic states in 2D layered magnetic materials. *Nat Rev Phys* 2019;1:646-61. DOI
75. Zhang S, Xu R, Luo N, Zou X. Two-dimensional magnetic materials: structures, properties and external controls. *Nanoscale* 2021;13:1398-424. DOI PubMed
76. Flem G, Brec R, Ouvard G, Louisy A, Segransan P. Magnetic interactions in the layer compounds MPX_3 (M = Mn, Fe, Ni; X = S,

Se). *Journal of Physics and Chemistry of Solids* 1982;43:455-61. DOI
77. Kim K, Lim SY, Lee JU, et al. Suppression of magnetic ordering in XXZ-type antiferromagnetic monolayer $NiPS_3$. *Nat Commun* 2019;10:345. DOI PubMed PMC
78. Menichetti G, Calandra M, Polini M. Electronic structure and magnetic properties of few-layer $Cr_2Ge_2Te_6$: the key role of nonlocal electron-electron interaction effects. *2D Mater* 2019;6:045042. DOI
79. Deiseroth H, Aleksandrov K, Reiner C, Kienle L, Kremer RK. Fe_3GeTe_2 and Ni_3GeTe_2 - two new layered transition - metal compounds: crystal structures, HRTEM investigations, and magnetic and electrical properties. *Eur J Inorg Chem* 2006;2006:1561-7. DOI
80. Yan J, Zhang Q, Heitmann T, et al. Crystal growth and magnetic structure of $MnBi_2Te_4$. *Phys Rev Materials* 2019:3. DOI
81. Xue Y, Zhang Y, Wang H, et al. Thickness-dependent magnetotransport properties in 1T VSe_2 single crystals prepared by chemical vapor deposition. *Nanotechnology* 2020;31:145712. DOI PubMed
82. Kim K, Lim SY, Kim J, et al. Antiferromagnetic ordering in van der Waals 2D magnetic material $MnPS_3$ probed by Raman spectroscopy. *2D Mater* 2019;6:041001. DOI
83. Yi J, Zhuang H, Zou Q, et al. Competing antiferromagnetism in a quasi-2D itinerant ferromagnet: Fe_3GeTe_2. *2D Mater* 2017;4:011005. DOI
84. Mcguire MA, Clark G, Kc S, et al. Magnetic behavior and spin-lattice coupling in cleavable van der Waals layered $CrCl_3$ crystals. *Phys Rev Materials* 2017:1. DOI
85. Qi H, Wang L, Sun J, et al. Production methods of Van der Waals heterostructures based on transition metal dichalcogenides. *Crystals* 2018;8:35. DOI
86. Adhikari S, Selvaraj S, Kim D. Progress in powder coating technology using Atomic layer deposition. *Adv Mater Interfaces* 2018;5:1800581. DOI
87. Nunn W, Truttmann TK, Jalan B. A review of molecular-beam epitaxy of wide bandgap complex oxide semiconductors. *J Mater Res* 2021;36:4846-64. DOI
88. Liu H, Xue Y, Shi JA, et al. Observation of the kondo effect in multilayer single-crystalline VTe_2 nanoplates. *Nano Lett* 2019;19:8572-80. DOI PubMed
89. Bagga V, Kaur D. Synthesis, magnetic ordering, transport studies on spintronic device heterostructures of 2D magnetic materials: a review. *Materials Today: Proceedings* 2020;28:1938-42. DOI
90. Jiang H, Zhang P, Wang X, Gong Y. Synthesis of magnetic two-dimensional materials by chemical vapor deposition. *Nano Res* 2021;14:1789-801. DOI
91. Liu S, Yuan X, Zou Y, et al. Wafer-scale two-dimensional ferromagnetic Fe_3GeTe_2 thin films grown by molecular beam epitaxy. *NPJ 2D Mater Appl* 2017:1. DOI
92. Huang P, Zhang P, Xu S, Wang H, Zhang X, Zhang H. Recent advances in two-dimensional ferromagnetism: materials synthesis, physical properties and device applications. *Nanoscale* 2020;12:2309-27. DOI PubMed
93. Wu M, Li Z, Cao T, Louie SG. Physical origin of giant excitonic and magneto-optical responses in two-dimensional ferromagnetic insulators. *Nat Commun* 2019;10:2371. DOI PubMed PMC
94. Gibertini M, Koperski M, Morpurgo AF, Novoselov KS. Magnetic 2D materials and heterostructures. *Nat Nanotechnol* 2019;14:408-19. DOI PubMed
95. Gong C. & Zhang, X. Two-dimensional magnetic crystals and emergent heterostructure devices. *Science* 2019; 363:eaav4450. DOI PubMed
96. Kitaev A. Anyons in an exactly solved model and beyond. *Ann Phys* 2006;321:2-111. DOI
97. Hikami S, Tsuneto T. Phase transition of quasi-two dimensional planar system. *Progress of Theoretical Physics* 1980;63:387-401. DOI
98. Kosterlitz JM, Thouless DJ. Ordering, metastability and phase transitions in two-dimensional systems. *J Phys C: Solid State Phys* 1973;6:1181-203. DOI PubMed
99. Iwashita T, Uryû N. Effects of biquadratic exchange in ferromagnets. *Phys Rev B* 1976;14:3090-6. DOI
100. Dzyaloshinsky I. A thermodynamic theory of "weak" ferromagnetism of antiferromagnetics. *Journal of Physics and Chemistry of Solids* 1958;4:241-55. DOI
101. Moriya T. Anisotropic superexchange interaction and weak ferromagnetism. *Phys Rev* 1960;120:91-8. DOI
102. Grechnev A, Irkhin VY, Katsnelson MI, Eriksson O. Thermodynamics of a two-dimensional Heisenberg ferromagnet with dipolar interaction. *Phys Rev B* 2005:71. DOI
103. Jiang P, Wang C, Chen D, et al. Stacking tunable interlayer magnetism in bilayer CrI3. *Phys Rev B* 2019:99. DOI
104. Kan M, Adhikari S, Sun Q. Ferromagnetism in MnX_2 (X = S, Se) monolayers. *Phys Chem Chem Phys* 2014;16:4990-4. DOI PubMed
105. Burch KS, Mandrus D, Park JG. Magnetism in two-dimensional van der Waals materials. *Nature* 2018;563:47-52. DOI PubMed
106. Liu J, Meng S, Sun JT. Spin-orientation-dependent topological states in Two-dimensional antiferromagnetic $NiTl_2S_4$ monolayers. *Nano Lett* 2019;19:3321-6. DOI PubMed
107. Bender SA, Duine RA, Tserkovnyak Y. Electronic pumping of quasiequilibrium Bose-Einstein-condensed magnons. *Phys Rev Lett* 2012;108:246601. DOI PubMed
108. Park T, Peng L, Liang J, et al. Néel-type skyrmions and their current-induced motion in van der Waals ferromagnet-based

heterostructures. *Phys Rev B* 2021:103. DOI

109. Jiang J, Liu X, Li R, Mi W. Topological spin textures in a two-dimensional $MnBi_2(Se,Te)_4$ Janus material. *Appl Phys Lett* 2021;119:072401. DOI
110. Jiang J, Li R, Mi W. Electrical control of topological spin textures in two-dimensional multiferroics. *Nanoscale* 2021;13:20609-14. DOI PubMed
111. Pervishko AA, Baglai MI, Eriksson O, Yudin D. Another view on Gilbert damping in two-dimensional ferromagnets. *Sci Rep* 2018;8:17148. DOI PubMed PMC
112. Afanasiev D, Hortensius JR, Matthiesen M, et al. Controlling the anisotropy of a van der Waals antiferromagnet with light. *Sci Adv* 2021;7:eabf3096. DOI PubMed PMC
113. Seyler KL, Zhong D, Klein DR, et al. Ligand-field helical luminescence in a 2D ferromagnetic insulator. *Nature Phys* 2018;14:277-81. DOI
114. Zhong D, Seyler KL, Linpeng X, et al. Van der Waals engineering of ferromagnetic semiconductor heterostructures for spin and valleytronics. *Sci Adv* 2017;3:e1603113. DOI PubMed PMC
115. Webster L, Liang L, Yan JA. Distinct spin-lattice and spin-phonon interactions in monolayer magnetic CrI_3. *Phys Chem Chem Phys* 2018;20:23546-55. DOI PubMed
116. Katanin A. Quantum critical behavior of antiferromagnetic itinerant systems with van Hove singularities. *Phys Rev B* 2010:81. DOI
117. Yazyev OV, Capaz RB, Louie SG. Theory of magnetic edge states in chiral graphene nanoribbons. *Phys Rev B* 2011:84. DOI
118. Seyler KL, Zhong D, Huang B, et al. Valley manipulation by optically tuning the magnetic proximity effect in WSe_2/CrI_3 heterostructures. *Nano Lett* 2018;18:3823-8. DOI PubMed
119. Dolui K, Pemmaraju CD, Sanvito S. Electric field effects on armchair MoS_2 nanoribbons. *ACS Nano* 2012;6:4823-34. DOI PubMed
120. Tian Y, Gao W, Henriksen EA, Chelikowsky JR, Yang L. Optically driven magnetic phase transition of monolayer $RuCl_3$. *Nano Lett* 2019;19:7673-80. DOI PubMed
121. Tian S, Zhang JF, Li C, et al. Ferromagnetic van der Waals crystal VI_3. *J Am Chem Soc* 2019;141:5326-33. DOI PubMed
122. Ersan F, Vatansever E, Sarikurt S, et al. Exploring the electronic and magnetic properties of new metal halides from bulk to two-dimensional monolayer: RuX_3 (X = Br, I). *Journal of Magnetism and Magnetic Materials* 2019;476:111-9. DOI
123. Tartaglia TA, Tang JN, Lado JL, et al. Accessing new magnetic regimes by tuning the ligand spin-orbit coupling in van der Waals magnets. *Sci Adv* 2020;6:eabb9379. DOI PubMed PMC
124. Zhang Z, Shang J, Jiang C, Rasmita A, Gao W, Yu T. Direct photoluminescence probing of ferromagnetism in monolayer two-dimensional $CrBr_3$. *Nano Lett* 2019;19:3138-42. DOI PubMed
125. Liu J, Sun Q, Kawazoe Y, Jena P. Exfoliating biocompatible ferromagnetic Cr-trihalide monolayers. *Phys Chem Chem Phys* 2016;18:8777-84. DOI PubMed
126. Ren Y, Li Q, Wan W, Liu Y, Ge Y. High-temperature ferromagnetic semiconductors: Janus monolayer vanadium trihalides. *Phys Rev B* 2020:101. DOI
127. Yaresko AN. Electronic band structure and exchange coupling constants in ACr_2X_4 spinels (A=Zn , Cd, Hg; X=O , S, Se). *Phys Rev B* 2008:77. DOI
128. Bedoya-Pinto A, Ji JR, Pandeya AK, et al. Intrinsic 2D-XY ferromagnetism in a van der Waals monolayer. *Science* 2021;374:616-20. DOI PubMed
129. Ubrig N, Wang Z, Teyssier J, et al. Low-temperature monoclinic layer stacking in atomically thin CrI_3 crystals. *2D Mater* 2019;7:015007. DOI
130. Torelli D, Olsen T. Calculating critical temperatures for ferromagnetic order in two-dimensional materials. *2D Mater* 2019;6:015028. DOI
131. Chen L, Chung J, Stone MB, et al. Magnetic Field Effect on Topological Spin Excitations in CrI_3. *Phys Rev X* 2021:11. DOI
132. Li R, Jiang J, Shi X, Mi W, Bai H. Two-dimensional Janus FeXY (X, Y = Cl, Br, and I, $X \neq Y$) monolayers: half-metallic ferromagnets with tunable magnetic properties under strain. *ACS Appl Mater Interfaces* 2021;13:38897-905. DOI
133. Qi S, Jiang J, Wang X, Mi W. Valley polarization, magnetic anisotropy and Dzyaloshinskii-Moriya interaction of two-dimensional graphene/Janus 2H-VSeX(X = S, Te) heterostructures. *Carbon* 2021;174:540-55. DOI
134. Fu L, Liu X, Zhou B, Wang X. Prediction of high spin polarization and perpendicular magnetic anisotropy in two dimensional ferromagnetic Mn2CXX' (X, X'=F, Cl, Br, I) Janus monolayers. *Physica E: Low-dimensional Systems and Nanostructures* 2021;134:114932. DOI
135. Zhang F, Mi W, Wang X. Spin-dependent electronic structure and magnetic anisotropy of 2D ferromagnetic janus Cr_2I_3. *X* ;6:1900778. DOI
136. Xu Y, Qi S, Mi W. Electronic structure and magnetic properties of two-dimensional h-BN/Janus 2H-VSe_X (X = S, Te) van der Waals heterostructures. *Applied Surface Science* 2021;537:147898. DOI
137. Li R, Jiang J, Mi W, Bai H. Room temperature spontaneous valley polarization in two-dimensional FeClBr monolayer. *Nanoscale* 2021;13:14807-13. DOI PubMed
138. Fu L, Wang X, Mi W. Spin-dependent electronic structure and magnetic properties of 2D JANUS $Mn_2CFCl/CuBiP_2$ Se_6 Van Der Waals multiferroic heterostructures. *Adv Theory Simul* 2021;4:2100302. DOI
139. Liang J, Wang W, Du H, et al. Very large Dzyaloshinskii-Moriya interaction in two-dimensional Janus manganese dichalcogenides and its application to realize skyrmion states. *Phys Rev B* 2020:101. DOI

140. Qi S, Jiang J, Mi W. Tunable valley polarization, magnetic anisotropy and Dzyaloshinskii-Moriya interaction in two-dimensional intrinsic ferromagnetic Janus 2H-VSe_X (X = S, Te) monolayers. *Phys Chem Chem Phys* 2020;22:23597-608. DOI PubMed
141. Son S, Coak MJ, Lee N, et al. Bulk properties of the van der Waals hard ferromagnet VI3. *Phys Rev B* 2019:99. DOI
142. Ramasubramaniam A, Naveh D. Mn-doped monolayer MoS_2: an atomically thin dilute magnetic semiconductor. *Phys Rev B* 2013:87. DOI
143. Yu W, Li J, Herng TS, et al. Chemically exfoliated VSe_2 monolayers with room-temperature ferromagnetism. *Adv Mater* 2019;31:e1903779. DOI PubMed
144. Lee S, Park TB, Kim J, et al. Tuning the charge density wave quantum critical point and the appearance of superconductivity in $TiSe_2$. *Phys Rev Research* 2021:3. DOI
145. Liu Z, Wu X, Shao Y, et al. Epitaxially grown monolayer VSe_2: an air-stable magnetic two-dimensional material with low work function at edges. *Science Bulletin* 2018;63:419-25. DOI
146. Wei S, Liao X, Wang C, et al. Emerging intrinsic magnetism in two-dimensional materials: theory and applications. *2D Mater* 2020;8:012005. DOI
147. Zhang W, Guo HT, Jiang J, et al. Magnetism and magnetocrystalline anisotropy in single-layer $PtSe_2$: interplay between strain and vacancy. *Journal of Applied Physics* 2016;120:013904. DOI
148. Zhang H, Fan X, Yang Y, Xiao P. Strain engineering the magnetic states of vacancy-doped monolayer $MoSe_2$. *Journal of Alloys and Compounds* 2015;635:307-13. DOI
149. Fuh H, Yan B, Wu S, Felser C, Chang C. Metal-insulator transition and the anomalous hall effect in the layered magnetic materials VS_2 and VSe_2. *New J Phys* 2016;18:113038. DOI
150. Mishra R, Zhou W, Pennycook SJ, Pantelides ST, Idrobo J. Long-range ferromagnetic ordering in manganese-doped two-dimensional dichalcogenides. *Phys Rev B* 2013:88. DOI
151. Wang Y, Li S, Yi J. Electronic and magnetic properties of Co doped MoS_2 monolayer. *Sci Rep* 2016;6:24153. DOI PubMed PMC
152. Shi M, Mo P, Lu J, Liu J. Strain-enhanced electron mobility and mobility anisotropy in a two-dimensional vanadium diselenide monolayer. *Journal of Applied Physics* 2019;126:044305. DOI
153. Wang Z, Zhang T, Ding M, et al. Electric-field control of magnetism in a few-layered van der Waals ferromagnetic semiconductor. *Nat Nanotechnol* 2018;13:554-9. DOI PubMed
154. Lee JU, Lee S, Ryoo JH, et al. Ising-type magnetic ordering in atomically thin $FePS_3$. *Nano Lett* 2016;16:7433-8. DOI PubMed
155. Chu H, Roh CJ, Island JO, et al. Linear magnetoelectric phase in ultrathin $MnPS_3$ probed by optical second harmonic generation. *Phys Rev Lett* 2020;124:027601. DOI PubMed
156. Wang Y, Zhang J, Li C, et al. Raman scattering study of magnetic layered MPS_3 crystals (M = Mn , Fe, Ni)*. *Chinese Phys B* 2019;28:056301. DOI
157. Long G, Henck H, Gibertini M, et al. Persistence of Magnetism in Atomically Thin $MnPS_3$ Crystals. *Nano Lett* 2020;20:2452-9. DOI PubMed
158. Liu S, Granados Del Águila A, Bhowmick D, et al. Direct observation of magnon-phonon strong coupling in two-dimensional antiferromagnet at high magnetic fields. *Phys Rev Lett* 2021;127:097401. DOI PubMed
159. Kim SY, Kim TY, Sandilands LJ, et al. Charge-spin correlation in van der Waals antiferromagnet NiPS_{3}. *Phys Rev Lett* 2018;120:136402. DOI PubMed
160. Haines CRS, Coak MJ, Wildes AR, et al. Pressure-induced electronic and structural phase evolution in the van der Waals compound FePS_{3}. *Phys Rev Lett* 2018;121:266801. DOI PubMed
161. Xu C, Feng J, Xiang H, Bellaiche L. Interplay between Kitaev interaction and single ion anisotropy in ferromagnetic CrI3 and CrGeTe3 monolayers. *npj Comput Mater* 2018:4. DOI
162. Baranava M, Hvazdouski D, Skachkova V, Stempitsky V, Danilyuk A. Magnetic interactions in $Cr_2Ge_2Te_6$ and $Cr_2Si_2Te_6$ monolayers: ab initio study. *Materials Today: Proceedings* 2020;20:342-7. DOI
163. Liu Y, Petrovic C. Critical behavior of quasi-two-dimensional semiconducting ferromagnet $Cr_2Ge_2Te_6$. *Phys Rev B* 2017:96. DOI
164. Feng YP, Shen L, Yang M, et al. Prospects of spintronics based on 2D materials. *WIREs Comput Mol Sci* 2017:7. DOI
165. Dong E, Liu B, Dong Q, et al. Effects of pressure on the structure and properties of layered ferromagnetic $Cr_2Ge_2Te_6$. *Physica B: Condensed Matter* 2020;595:412344. DOI
166. Song C, Liu X, Wu X, et al. Surface-vacancy-induced metallicity and layer-dependent magnetic anisotropy energy in $Cr_2Ge_2Te_6$. *J Appl Phys* 2019;126:105111. DOI
167. Liu W, Wang Y, Han Y, et al. Anisotropic magnetoresistance behaviors in the layered ferromagnetic $Cr_2Ge_2Te_6$. *J Phys D: Appl Phys* 2020;53:025101. DOI
168. Wang N, Tang H, Shi M, et al. Transition from ferromagnetic semiconductor to ferromagnetic metal with enhanced curie temperature in $Cr_2Ge_2Te_6$ via organic ion intercalation. *J Am Chem Soc* 2019;141:17166-73. DOI PubMed
169. Fang Y, Wu S, Zhu Z, Guo G. Large magneto-optical effects and magnetic anisotropy energy in two-dimensional $Cr_2Ge_2Te_6$. *Phys Rev B* 2018:98. DOI
170. Han MG, Garlow JA, Liu Y, et al. Topological magnetic-spin textures in two-dimensional van der Waals $Cr_2Ge_2Te_6$. *Nano Lett* 2019;19:7859-65. DOI PubMed
171. Tian Y, Gray MJ, Ji H, Cava RJ, Burch KS. Magneto-elastic coupling in a potential ferromagnetic 2D atomic crystal. *2D Mater* 2016;3:025035. DOI

172. Zhuang HL, Kent PRC, Hennig RG. Strong anisotropy and magnetostriction in the two-dimensional Stoner ferromagnet Fe3GeTe2. *Phys Rev B* 2016:93. DOI
173. Tong Q, Chen M, Yao W. Magnetic proximity effect in a van der Waals Moiré superlattice. *Phys Rev Applied* 2019:12. DOI
174. Qi X, Zhang S. Topological insulators and superconductors. *Rev Mod Phys* 2011;83:1057-110. DOI
175. Mogi M, Tsukazaki A, Kaneko Y, et al. Ferromagnetic insulator $Cr_2Ge_2Te_6$ thin films with perpendicular remanence. *APL Materials* 2018;6:091104. DOI
176. Tan C, Lee J, Jung SG, et al. Hard magnetic properties in nanoflake van der Waals Fe_3GeTe_2. *Nat Commun* 2018;9:1554. DOI PubMed PMC
177. Wang H, Xu R, Liu C, et al. Pressure-dependent intermediate magnetic phase in thin Fe_3GeTe_2 flakes. *J Phys Chem Lett* 2020;11:7313-9. DOI PubMed
178. May AF, Calder S, Cantoni C, Cao H, Mcguire MA. Magnetic structure and phase stability of the van der Waals bonded ferromagnet Fe3-xGeTe2. *Phys Rev B* 2016:93. DOI
179. Fei Z, Huang B, Malinowski P, et al. Two-dimensional itinerant ferromagnetism in atomically thin Fe_3GeTe_2. *Nat Mater* 2018;17:778-82. DOI PubMed
180. Li Q, Yang M, Gong C, et al. Patterning-induced ferromagnetism of Fe_3GeTe_2 van der Waals materials beyond room temperature. *Nano Lett* 2018;18:5974-80. DOI PubMed
181. Hu X, Zhao Y, Shen X, Krasheninnikov AV, Chen Z, Sun L. Enhanced ferromagnetism and tunable magnetism in Fe_3GeTe_2 monolayer by strain engineering. *ACS Appl Mater Interfaces* 2020;12:26367-73. DOI PubMed
182. Zhang Y, Lu H, Zhu X, et al. Emergence of Kondo lattice behavior in a van der Waals itinerant ferromagnet, Fe_3GeTe_2. *Sci Adv* 2018;4:eaao6791. DOI PubMed PMC
183. Zhao M, Chen BB, Xi Y, et al. Kondo holes in the two-dimensional itinerant ising ferromagnet Fe_3GeTe_2. *Nano Lett* 2021;21:6117-23. DOI PubMed
184. Wang Y, Chen X, Long M. Modifications of magnetic anisotropy of Fe_3GeTe_2 by the electric field effect. *Appl Phys Lett* 2020;116:092404. DOI
185. Lin H, Yan F, Hu C, et al. Current-assisted magnetization reversal in Fe_3GeTe_2 van der Waals homojunctions. *Nanoscale* 2022;14:2352-8. DOI PubMed
186. Wu Q, Ang YS, Cao L, Ang LK. Design of metal contacts for monolayer Fe_3GeTe_2 based devices. *Appl Phys Lett* 2019;115:083105. DOI
187. Krstajić P, Peeters F, Ivanov V, Fleurov V, Kikoin K. Double-exchange mechanisms for Mn-doped III-V ferromagnetic semiconductors. *Phys Rev B* 2004:70. DOI
188. Wang H, Wang C, Li Z, et al. Characteristics and temperature-field-thickness evolutions of magnetic domain structures in van der Waals magnet Fe_3GeTe_2 nanolayers. *Appl Phys Lett* 2020;116:192403. DOI
189. Li J, Li Y, Du S, et al. Intrinsic magnetic topological insulators in van der Waals layered $MnBi_2Te_4$-family materials. *Sci Adv* 2019;5:eaaw5685. DOI PubMed PMC
190. Zhou Y, Wu MW. Electron spin relaxation in graphene from a microscopic approach: role of electron-electron interaction. *Phys Rev B* 2010:82. DOI
191. Soriano D, Katsnelson MI, Fernández-Rossier J. Magnetic two-dimensional chromium trihalides: a theoretical perspective. *Nano Lett* 2020;20:6225-34. DOI PubMed
192. Ningrum VP, Liu B, Wang W, et al. Recent advances in two-dimensional magnets: physics and devices towards spintronic applications. *Research (Wash D C)* 2020;2020:1768918. DOI PubMed PMC
193. Javaid M, Taylor PD, Tawfik SA, Spencer MJS. Tuning the Schottky barrier height in a multiferroic In_2Se_3/Fe_3GeTe_2 van der Waals heterojunction. *Nanoscale* 2022;14:4114-22. DOI PubMed
194. Kamerbeek AM, Ruiter R, Banerjee T. Large room-temperature tunneling anisotropic magnetoresistance and electroresistance in single ferromagnet/Nb:$SrTiO_3$ Schottky devices. *Sci Rep* 2018;8:1378. DOI PubMed PMC
195. Xi Z, Ruan J, Li C, et al. Giant tunnelling electroresistance in metal/ferroelectric/semiconductor tunnel junctions by engineering the Schottky barrier. *Nat Commun* 2017;8:15217. DOI PubMed PMC
196. Zhu R, Zhang W, Shen W, et al. Exchange bias in van der Waals $CrCl_3/Fe_3GeTe_2$ heterostructures. *Nano Lett* 2020;20:5030-5. DOI PubMed
197. He QL, Hughes TL, Armitage NP, Tokura Y, Wang KL. Topological spintronics and magnetoelectronics. *Nat Mater* 2022;21:15-23. DOI PubMed
198. Cai R, Yao Y, Lv P, et al. Evidence for anisotropic spin-triplet Andreev reflection at the 2D van der Waals ferromagnet/superconductor interface. *Nat Commun* 2021;12:6725. DOI PubMed PMC
199. Kezilebieke S, Huda MN, Dreher P, et al. Electronic and magnetic characterization of epitaxial VSe_2 monolayers on superconducting $NbSe_2$. *Commun Phys* 2020:3. DOI
200. Alegria LD, Ji H, Yao N, Clarke JJ, Cava RJ, Petta JR. Large anomalous Hall effect in ferromagnetic insulator-topological insulator heterostructures. *Appl Phys Lett* 2014;105:053512. DOI
201. Hejazi K, Luo ZX, Balents L. Noncollinear phases in moiré magnets. *Proc Natl Acad Sci U S A* 2020;117:10721-6. DOI PubMed PMC
202. Balents L, Dean CR, Efetov DK, Young AF. Superconductivity and strong correlations in moiré flat bands. *Nat Phys* 2020;16:725-

33. DOI
203. Tong Q, Liu F, Xiao J, Yao W. Skyrmions in the Moiré of van der Waals 2D magnets. *Nano Lett* 2018;18:7194-9. DOI PubMed
204. Cardoso C, Soriano D, García-Martínez NA, Fernández-Rossier J. Van der Waals spin valves. *Phys Rev Lett* 2018;121:067701. DOI PubMed
205. Song T, Tu MW, Carnahan C, et al. Voltage control of a van der Waals spin-filter magnetic tunnel junction. *Nano Lett* 2019;19:915-20. DOI PubMed
206. Lin H, Yan F, Hu C, et al. Spin-valve effect in $Fe_3GeTe_2/MoS_2/Fe_3GeTe_2$ van der Waals heterostructures. *ACS Appl Mater Interfaces* 2020;12:43921-6. DOI PubMed
207. Gennes P. Coupling between ferromagnets through a superconducting layer. *Physics Letters* 1966;23:10-1. DOI
208. Fukami S, Anekawa T, Zhang C, Ohno H. A spin-orbit torque switching scheme with collinear magnetic easy axis and current configuration. *Nat Nanotechnol* 2016;11:621-5. DOI PubMed
209. Wang X, Tang J, Xia X, et al. Current-driven magnetization switching in a van der Waals ferromagnet Fe_3GeTe_2. *Sci Adv* 2019;5:eaaw8904. DOI PubMed PMC
210. Johansen Ø, Risinggård V, Sudbø A, Linder J, Brataas A. Current control of magnetism in two-dimensional Fe_3GeTe_2. *Phys Rev Lett* 2019;122:217203. DOI PubMed